

Rice *Undeveloped Tapetum1* Is a Major Regulator of Early Tapetum Development ^W

Ki-Hong Jung,^a Min-Jung Han,^a Yang-Seok Lee,^a Yong-Woo Kim,^b Inhwan Hwang,^b Min-Jeong Kim,^c Yeon-Ki Kim,^c Baek Hie Nahm,^c and Gynheung An^{a,d,1}

^aNational Research Laboratory of Plant Functional Genomics, Division of Molecular and Life Sciences, Pohang University of Science and Technology, Pohang 790-784, Republic of Korea

^bCenter for Plant Intracellular Trafficking and Division of Molecular and Life Sciences, Pohang University of Science and Technology, Pohang 790-784, Republic of Korea

^cGreenGene Biotech, Myongji University 38-2, Namdong Yongin, Kyonggido 449-728, Republic of Korea

^dFunctional Genomic Center, Pohang University of Science and Technology, Pohang 790-784, Republic of Korea

The tapetum, the innermost of four sporophytic layers in the anther wall, comes in direct contact with the developing male gametophyte and is thought to play a crucial role in the development and maturation of microspores. Here, we report the identification of rice (*Oryza sativa*) *Undeveloped Tapetum1* (*Udt1*), which is required for the differentiation of secondary parietal cells to mature tapetal cells. *T-DNA* or retrotransposon *Tos17* insertions in the *Udt1* gene caused male sterility. The anther walls and meiocytes of the mutants were normal during the early premeiosis stage, but their tapeta failed to differentiate and became vacuolated during the meiotic stage. In addition, meiocytes did not develop to microspores, and middle layer degeneration was inhibited. Consequently, the anther locules contained no pollen. The UDT1:green fluorescent protein fusion protein was localized to the nucleus. This, together with its homology with other basic helix-loop-helix proteins, suggests that UDT1 is a transcription factor. DNA microarray analysis identified 958 downregulated and 267 upregulated genes in the *udt1-1* anthers, suggesting that *Udt1* plays a major role in maintaining tapetum development, starting in early meiosis.

INTRODUCTION

In angiosperm species, the floral meristem comprises three layers of cells with separate lineages: L1 (epidermis), L2 (sub-epidermis), and L3 (core) (Goldberg et al., 1993). During early anther development, archesporial cell division in the L2 gives rise to primary parietal cells and primary sporogenous cells (Scott et al., 2004). The primary sporogenous cell undergoes a small number of divisions to generate the meiocytes, which produce a tetrad of haploid cells that are released as free microspores (McCormick, 1993). The primary parietal cell divides periclinally to form an endothelial cell subjacent to the L1 and a secondary parietal cell. The latter again divides periclinally to generate a middle layer cell next to the endothecium and a tapetal cell adjacent to the sporogenous cells (Scott et al., 2004).

During microgametogenesis, microspores develop into mature pollen by two mitotic divisions. The innermost cell layer of the anther wall, the tapetum, plays a crucial role in supplying nutrients to the microspores and in regulating their release. Therefore, mutations affecting tapetum development lead to

aborted microgametogenesis and male sterility (Chaudhury, 1993; Wilson et al., 2001; Kapoor et al., 2002; Sorensen et al., 2002, 2003; Higginson et al., 2003).

Several genes that control the early stages of anther development have been identified through mutant analyses. For example, in *male sterile converted anther1* of maize (*Zea mays*), archesporial cells do not divide into primary sporogenous cells and primary parietal cells, and no microsporangia are formed (Chaubal et al., 2003). The *Arabidopsis thaliana* *NOZZLE/SPOROCYTELESS* (*NZZ/SPL*) gene product plays an important role in early anther development because the *nzz/spl* mutation blocks the differentiation of primary sporogenous cells into microspores as well as anther wall formation (Schiefthaler et al., 1999; Yang et al., 1999b). *NZZ/SPL* encodes a putative MADS-related transcription factor; its expression is restricted to developing microsporocytes in the anther. A defect in *EXCESS MICROSPOROCTES1* (*EMS1*) generates extra meiocytes but lacks tapetal and middle layers (Canales et al., 2002; Zhao et al., 2002). Mutation in *TAPETUM DETERMINANT1* (*TPD1*) fails to specialize tapetal cell fate during the progression from secondary parietal cells to the tapetal and middle layers (Yang et al., 2003a). As a result, extra microsporocytes are formed and the tapetum is absent in the *tpd1* anthers. The *TPD1* product plays an important role in the differentiation of tapetal cells, possibly in coordination with the *EMS1* product, because *tpd1* was phenotypically similar to *ems1* single and *tpd1 ems1* double mutants (Yang et al., 2003a).

Finally, the necessity of *MULTIPLE SPOROCTE1* (*MSP1*), which encodes a Leu-rich repeat receptor-like protein, has been

¹To whom correspondence should be addressed. E-mail genean@postech.ac.kr; fax 82-54-279-0659.

The authors responsible for distribution of materials integral to the findings presented in this article in accordance with the policy described in the Instructions for Authors (www.plantcell.org) are: Ki-Hong Jung (jkhim@postech.ac.kr) and Gynheung An (genean@postech.ac.kr).

^WOnline version contains Web-only data.

Article, publication date, and citation information can be found at www.plantcell.org/cgi/doi/10.1105/tpc.105.034090.

demonstrated for early sporogenic development and the initiation of anther wall formation in rice (*Oryza sativa*) (Nonomura et al., 2003). The *msp1* mutation gives rise to an excessive number of both male and female sporocytes, resulting in complete male sterility. In addition, genes associated with meiosis have been identified (Glover et al., 1998; Yang et al., 1999a, 2003b; Armstrong et al., 2002; Azumi et al., 2002; Nonomura et al., 2004b).

Some mutations affect the development of the tapetum and microspores. For instance, those of the *Arabidopsis* *MALE STERILITY2 (MS2)* gene, which is homologous with fatty acyl reductase, cause defective pollen wall formation at the stage when microspores are released from the tetrads (Aarts et al., 1997). Mutations in *Arabidopsis* *ABORTED MICROSPORE (AMS)* containing a basic helix-loop-helix (bHLH) domain, in *MS1* genes homologous with the PHD-finger family, and in *Petunia hybrida* *TAPETUM DEVELOPMENT ZINC FINGER PROTEIN1* show defects in tapetum development after microsporogenesis. All three proteins are predicted to function as transcription factors (Wilson et al., 2001; Kapoor et al., 2002; Sorensen et al., 2003).

Cytological analyses of anther development in cereals such as maize and rice showed that the morphological characteristics of anther development are similar to those of dicots (Sanders et al., 1999; Chaubal et al., 2003). However, adaptations to environmental stresses are quite different (Imin et al., 2004). Around the time when pollen mother cells enter the reproductive division stage, rice anthers are adversely affected by low-temperature treatment (<20°C). The cold stress causes tapetal cells to swell; consequently, pollen mother cells cannot receive nutrients and die. Moisture shortage also exerts an adverse effect on the development of anther and pollen grains.

Despite its importance in crop yield and hybrid seed production, studies of anther development in cereal plants are rare. Because the rice genome sequence has been determined and a large number of insertional mutants are available, rice is an excellent model plant for cereal developmental biology (An et al., 2005; Sasaki et al., 2005). To this end, we screened for male-sterile mutants from rice using T-DNA insertional lines that were generated previously (Jeon et al., 2000; Jeong et al., 2002; Jung et al., 2003; Lee et al., 2003, 2004; Ryu et al., 2004). The T-DNA carries the β -glucuronidase (*GUS*) reporter gene that creates a fusion with an endogenous gene, thereby allowing tagged genes to be detected via *GUS* assays. Among the *GUS*-positive lines here, we studied an anther-defective mutant with a T-DNA insertion in a putative transcription factor containing the bHLH domain.

The bHLH protein belongs to the MYC class family that contains *AMS* and *INDUCED OF CBF EXPRESSION1 (ICE1)* (Chinnusamy et al., 2003; Sorensen et al., 2003; Toledo-Ortiz et al., 2003). In mammals, *MYC* (for *Myc proto-oncogene protein*) genes influence a variety of cellular processes, including growth, metabolism, cell cycle progression, signal transduction, and apoptosis (Coller et al., 2000). MYC proteins activate transcription as obligate heterodimers with a partner protein, MYC-ASSOCIATED FACTOR X (MAX), which carries the bHLH domain. The MYC-MAX complex binds to E-box DNA elements with the core sequence CANNTG (Bouchard et al., 1998; Chinnusamy et al., 2003). In *Arabidopsis*, a bHLH protein, *LONG HYPOCOTYL IN FAR-RED1*, can form both homodimers and heterodimers with the closely related *PHYTOCHROME INTERACTING FACTOR3*

protein (Fairchild et al., 2000). Recently, interactions between bHLH and MYB proteins have been described (Abe et al., 2003; Baudry et al., 2004). In this report, we describe the role of *Undeveloped Tapetum1 (Udt1)* on early tapetum development. Identification of the *Udt1* gene and putative downstream genes is an important step toward understanding anther development in rice and developing crop plants that are more tolerant of environmental stresses.

RESULTS

Isolation of Male-Sterile Mutants from T-DNA-Tagged Lines

We conducted *GUS* assays of the developing flowers from 14,000 rice plants that had been generated by T-DNA insertional mutagenesis. A total of 270 lines were found that showed preferential *GUS* activity in their anthers. Phenotypic analysis of these *GUS*-positive lines identified 15 male-sterile lines, in which the mutant phenotype cosegregated with *GUS*.

Here, we report the detailed analysis of one line, 9-142-08. In the T2 progeny, the *GUS*-positive to *GUS*-negative ratio was 3:1. Although approximately two-thirds of the former plants were fertile, the remaining one-third were sterile as a result of the lack of mature pollen grains. T3 progeny from the *GUS*-positive fertile plants had the same 3:1 ratio, again, with one-third of the *GUS*-positive plants being male-sterile. We named this mutant *udt1*.

In the developing spikelets of heterozygous plants, *GUS* activity was detectable mainly in the anthers, with the level being high during tapetal development but decreasing after tapetum degeneration (Figures 1A to 1C). Before the initiation of tapetum development, we could not detect *GUS* expression in anthers at the early premeiosis stage (Figure 1A, left), but *GUS* activity was weakly detected in anthers at the late premeiosis stage (Figure 1A, right). In the ovary and awn, *GUS* activity was detected at low levels (Figure 1D), but it was not detected in the other floral organs. Also, *GUS* was not expressed in the other vegetative organs (data not shown). Cross sections of anthers at the late premeiosis and meiosis stages revealed *GUS* activity in both the anther wall and the microspore (Figures 1E and 1F). After meiosis, *GUS* activity was detected in the tapetum, connective tissue, and vascular bundles but not in the young microspores (Figure 1G). In the male-sterile anthers, the *GUS* expression pattern was similar to that seen in fertile anthers during meiosis. After meiosis, the tapetal cells in the mutant anthers were swollen. These tapetal cells and degenerated microspores were heavily stained by *GUS* (Figure 1H).

Sequence Analysis of the T-DNA-Tagged Gene

We amplified the flanking region of the inserted T-DNA in line 9-142-08 by thermal asymmetric interlaced (TAIL)-PCR. Sequence analysis of that region revealed that T-DNA was inserted into a gene located on chromosome 7 in P1 ARTIFICIAL CHROMOSOME clone P0534A03. This coding region was identified by RT-PCR and the Rice Genome Automated Annotation System (GAAS; <http://ricegaas.dna.affrc.go.jp/>). Its primary structure comprises four exons and three introns (Figure 2A). An EST

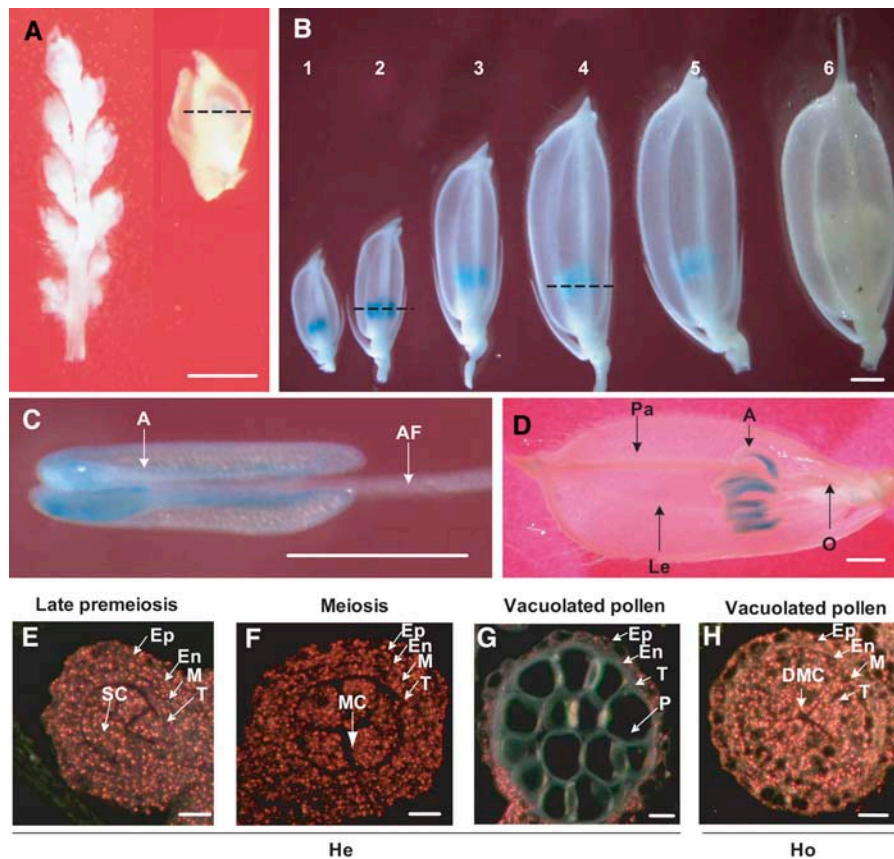


Figure 1. Expression Profiles of *Udt1* Using the GUS Assay.

(A) Expression pattern of the *Udt1:GUS* fusion product in heterozygous spikelets before meiosis: early premeiosis stage (left) and late premeiosis stage (right).

(B) Temporal and spatial expression patterns of the *Udt1:GUS* fusion product in heterozygous spikelets at various flowering stages. Sample 1, meiosis; 2, tetrad; 3, early young microspore; 4, late young microspore; 5, vacuolated pollen; 6, late pollen mitosis.

(C) Anther at the vacuolated pollen stage magnified.

(D) Photograph taken after the removal of half of the palea and lemma from a spikelet at the vacuolated pollen stage.

(E) to (G) Cross sections of *Udt1:GUS* heterozygous spikelets at late premeiosis, meiosis, and the vacuolated pollen stage, respectively.

(H) Cross section of a homozygous anther at the vacuolated pollen stage.

Photographs in **(E) to (H)** were taken with a dark-field microscope. GUS activity under the dark field appeared as pink or red colors. A, anther; AF, anther filament; DMC, degenerated meiocyte; En, endothelial cell layer; Ep, epidermal cell layer; He, heterozygous plants; Ho, knockout plants; Le, lemma; M, middle layer; MC, meiocyte; O, ovary; P, pollen; Pa, palea; SC, sporogenous cell; T, tapetal cell layer. Bars = 1 mm in **(A) to (D)** and 10 μm in **(E) to (H)**.

for this gene is not present in the National Center for Biotechnology Information (NCBI) database, suggesting that its expression is not strong or ubiquitous. In the *udt1* mutant allele (*udt1-2*), the T-DNA insertion was located at 1006 bp downstream from the ATG start codon, in the second intron of the gene.

The *Udt1* gene encodes a predicted protein of 227 amino acids (Figure 2B). The protein has an apparent molecular mass of 24.9 kD and a pI of 6.5. BLAST analysis indicated that the most similar proteins are the *Brassica napus* bHLH transcription factor CAD54298 and the *Arabidopsis* bHLH protein AMS (At2g16910), each of which shares 32% overall identity with the rice protein. AMS is known to be important for tapetum development (Sorensen et al., 2003). Also, UDT1 showed 31% identity with At1g10610 and 30% with ICE1, the overexpression of which improves freezing tolerance in transgenic plants (Chinnusamy

et al., 2003). Most *Arabidopsis* bHLH proteins that showed high identity with UDT1 belong to the group 9 bHLH protein family (Toledo-Ortiz et al., 2003). Functional domain analysis indicated that the region between the 59th and 118th amino acids is predicted to be a bHLH domain, possessing both the HLH domain required for dimerization and a nearby basic domain necessary for target DNA binding (Figure 2B). Multiple alignments showed well-conserved regions of four Leu residues important in forming an α -helix as well as nearby basic amino acid residues that are probably involved in DNA binding (Figure 2B).

The promoter region comprises a putative TATA box sequence at 406 bp upstream from the start ATG codon and a CAAT box sequence at -471. The upstream region also contains putative regulatory sequences: GTGA motifs (GTGA) at -485 and -48,

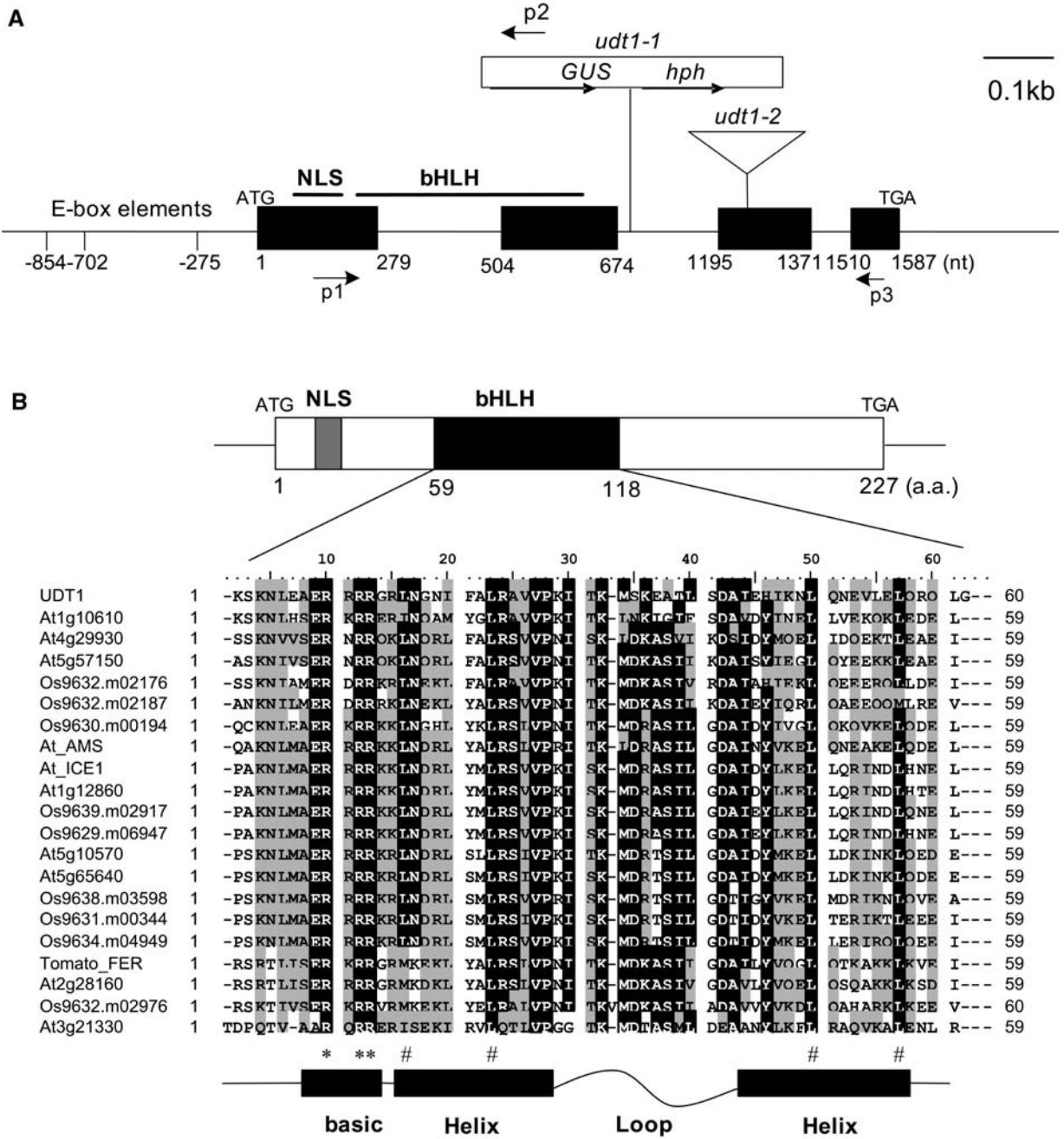


Figure 2. Scheme of the *Udt1* Gene and Multiple Alignment.

(A) Scheme of the *Udt1* gene and relative insertion positions of T-DNA and *Tos17*. Black boxes represent exons, and intervening lines represent introns. The ATG start codon and TGA stop codon are indicated. Insertion positions of T-DNA in line 9-142-08 (open box) and *Tos17* in line 1B-31-11 (triangle) are indicated at top. Number 1 indicates the starting nucleotide of translation, and 1587 indicates the nucleotide (nt) length from ATG to TGA. p1, p2, and p3 are primers for genotyping or identifying fusion transcripts between *Udt1* and *GUS*. Numbers -845, -702, and -205 indicate E-box sequences (the CANNTG motif) present upstream of ATG. bHLH, basic helix loop helix domain (amino acids 59 to 118); *hph*, hygromycin resistance marker for selection of the T-DNA insertion; NLS, nuclear localization signal (amino acids 3 to 17). Bar = 0.1 kb.

(B) Alignment of bHLH domains. The UDT1 protein was aligned with bHLH domains of the group 9 bHLH subfamily. Black boxes indicate amino acid (a.a.) residues that are >60% conserved, and gray boxes indicate amino acids that are >30% conserved. Asterisks indicate the conserved basic amino acid Arg that is important for binding DNA. Pound signs indicate conserved Leu residues important for forming the α -helix.

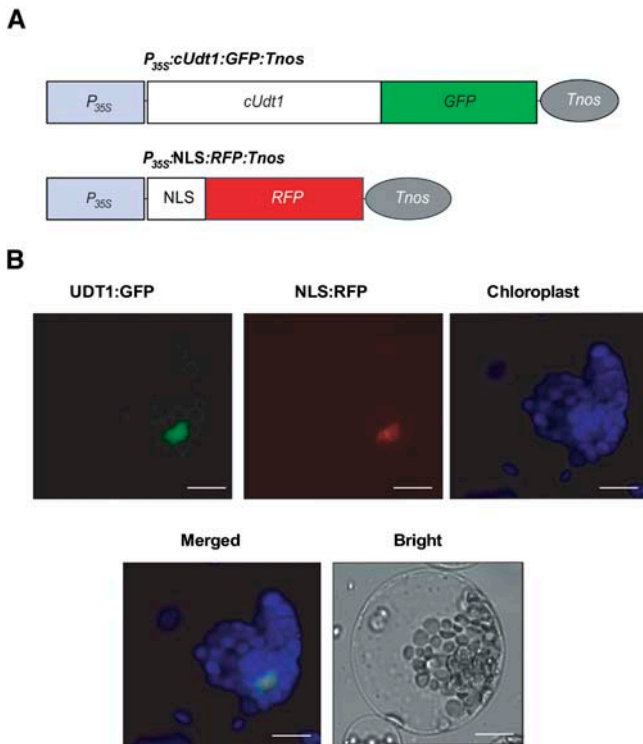


Figure 3. Subcellular Localization of UDT1.

(A) Schemes of fusion constructs. *p35S*, cauliflower mosaic virus 35S promoter; *cUdt1*, *Udt1* cDNA; *Tnos*, *nopaline synthase* gene terminator. (B) In vivo targeting of fusion proteins. Protoplasts were transformed with *P35S:cUdt1:GFP:Tnos* or *P35S:NLS:RFP:Tnos*; green and red fluorescent signals were examined 24 to 30 h after transformation. Data are representative of transformed protoplasts. At least two independent transformation experiments were performed with each construct. Note that the autofluorescent signal of chlorophyll is blue. "Merged" indicates that the green, red, and autofluorescent signals were merged. Bars = 20 μ m.

responsible for pollen specificity; E-box sequences (CANNTG) at -845 , -702 , and -205 , where the MYC class transcription factors bind; a MYBCORE motif (CNGTTR) at -238 , in which a petunia MYB protein involved in the regulation of flavonoid biosynthesis also binds (Solano et al., 1995); and a MYBGA motif (TAACAAA) at -945 , at which GAMYB binds.

UDT1 Is a Nuclear Protein

Because the previously characterized bHLH proteins are transcription factors, UDT1 may also be localized to the nucleus. The P-sort program (<http://bioweb.pasteur.fr/seqanal/interfaces/psort2.html>) supports the belief that UDT1 is a nuclear protein. To confirm this nuclear localization, we made a fusion between the *green fluorescent protein* (*GFP*) gene and *Udt1*; this construct was transiently expressed under the control of the 35S promoter and the *nos* terminator (Figure 3A). As a positive control, the previously characterized nuclear localization signal (NLS) of the B42 protein was fused to red fluorescent protein (RFP), and the fusion protein was expressed using the same regulatory elements. When chimeric molecules were introduced into

Arabidopsis protoplasts prepared from whole seedlings, we found that the UDT1:GFP was indeed localized to the nucleus (Figure 3B). The GFP signal coincided with an RFP signal driven by the NLS:RFP protein, indicating that UDT1 is a nuclear protein and can function as a transcriptional regulator.

Udt1 Transcript Is Most Abundant in Anthers during Early Developmental Stages

Because *Udt1* transcript levels were very low, it was difficult to elucidate the degree of expression by RNA gel blot analysis. Therefore, we performed semiquantitative RT-PCR with total RNA prepared from seedlings, panicles, and developing seeds. Transcript was detectable after 38 cycles of PCR. To recognize these low levels of expression, the PCR products were separated, blotted, and hybridized with a radiolabeled gene-specific probe. The *Udt1* gene was expressed at low levels in 7-d-old seedlings but at higher levels in the developing panicles (Figure 4A).

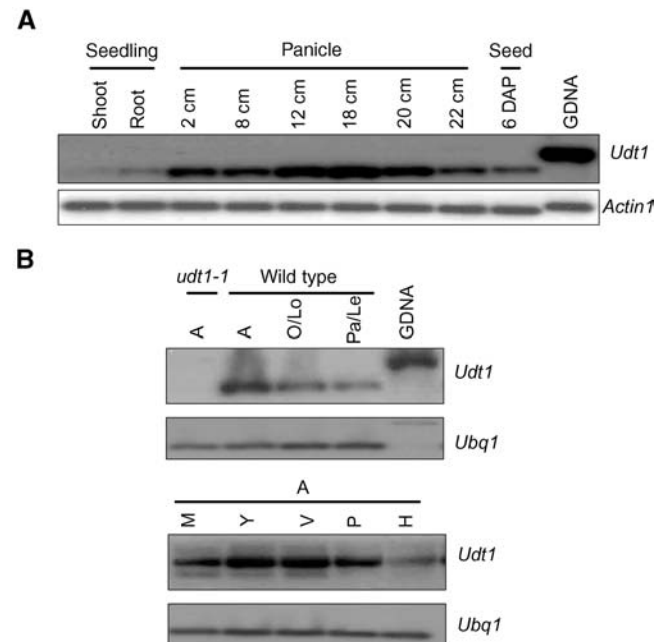


Figure 4. Expression Patterns of *Udt1* by Semiquantitative RT-PCR Analyses.

Primers were located on different exons; therefore, PCR products of cDNA were shorter than the genomic DNA product.

(A) Temporal expression patterns of *Udt1* in 7-d-old seedlings, at various stages of panicle formation, and in developing seeds 6 d after pollination. *Actin1* (Os03g50890) was used as a control.

(B) Top panel, spatial expression patterns of *Udt1* in developing spikelets. Anthers at meiosis to the young microspore stage were harvested from *udt1-1* and wild-type spikelets. Wild-type samples were also prepared from lodicules/ovaries and paleas/lemmas. Bottom panel, temporal expression patterns of *Udt1* in developing anthers at five different stages. *Ubiquitin extension protein1* (*Ubq1*; Os03g13170) was used as a control. Representative results from at least three replicates are shown for each panel. A, anther; O, ovary; Lo, lodicule; Pa, palea; Le, lemma; GDNA, genomic DNA; M, meiosis; Y, young microspore; V, vacuolated pollen; P, pollen mitosis; H, heading stage.

This gene was also expressed in developing seeds at 6 d after pollination. In the spikelets, the transcript level was higher in anthers than in other floral organs (Figure 4B). During anther development, the gene was more active at the early stages and only weakly active during heading (Figure 4B). As expected, *Udt1* transcript was not detectable in *udt1-1* anthers (Figure 4B).

Identification of an Additional *udt1* Allele Generated by a *Tos17* Insertion

To find any additional alleles of *udt1*, we screened our T-DNA insertional population. We reported previously that PCR can be used to identify T-DNA insertions from DNA pools (Lee et al., 2003). Our initial screening of 20,000 lines by T-DNA primers was

unsuccessful. Nevertheless, because we had earlier found an average of four new copies of *Tos17* in T-DNA insertional plants (Jeon et al., 2000), we screened the DNA pools with *Tos17* primers. This resulted in the identification of the *udt1-2* allele in line 1B-031-11, in which *Tos17* was inserted into the third exon of *Udt1* (Figure 2A). Plants homozygous for the *udt1-2* allele showed the same male-sterile phenotype as did the *udt1* mutant plants (data not shown). This mutant phenotype was cosegregated with the *udt1-2* allele, whereas *Udt1* transcript was absent in the homozygous plants.

Characterization of the *udt1* Mutant

Our homozygous *udt1-1* plants were completely male-sterile (Figures 5A to 5C). The mutant anthers were white because

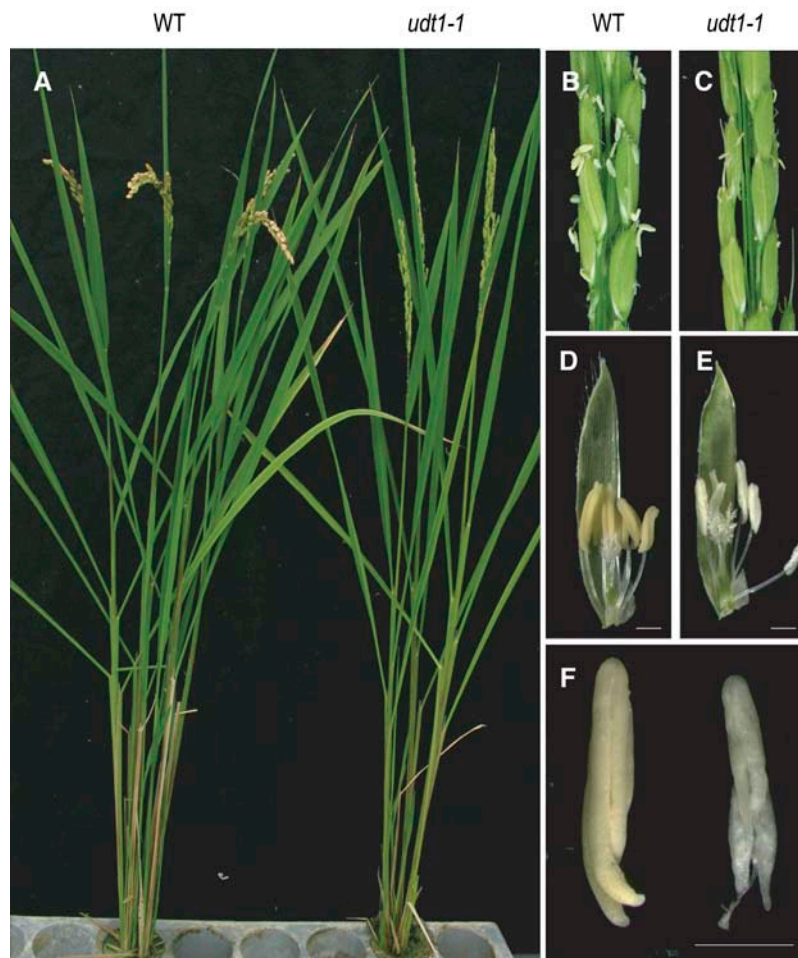


Figure 5. Phenotype of the *udt1* Knockout Plant.

- (A) Comparison of a wild-type plant (left) and a *udt1* knockout plant (right) after bolting.
 (B) Wild-type panicle at the heading stage.
 (C) *udt1* knockout panicle at the heading stage.
 (D) Wild-type spikelet after removal of the palea.
 (E) *udt1-1* spikelet after removal of the palea.
 (F) Comparison of a wild-type anther with a *udt1-1* anther at the pollen mitosis stage.
 Bars = 1 mm.

they lacked mature pollen grains, and the panicles failed to produce fertile seeds (Figures 5D to 5F). This sterile phenotype segregated as a single recessive mutation (fertile:sterile = 63:18, $\chi^2 = 0.25$ for 3:1 ratio).

We used pollen formation to delineate anther development into six stages for the wild-type panicles. During the early premeiosis stage (Figures 6A and 6G), the archesporoids divided to secondary parietal cells and sporogenous cells. Then, those secondary cells divided to inner (tapetal) layer cells and middle layer cells. During meiosis (Figures 6B and 6H), the sporogenous cells developed into pollen mother cells, which underwent meiosis to form tetrads of haploid microspores. The tapetal cells then differentiated and the middle layer cells degenerated. During the tetrad stages (Figures 6C and 6I), the meiocytes formed tetrads and free microspores were released into the anther locule. At the young microspore stage (Figures 6D and 6J), the microspores developed and exines were deposited. The middle layers then narrowed and the tapetal cell layers became very dense and thick. At the vacuolated stage (Figures 6E and 6K), the microspores finished their exine deposition and began to enrich the

pollen cytoplasm. During this process, the tapetal cells both differentiated and degenerated. At the pollen mitosis stage (Figures 6F and 6L), the uninucleate pollen developed to trinucleate pollen through two mitotic divisions. Simultaneously, starches, proteins, lipids, and other nutrients enriched the pollen cytoplasm. Tapetal cells were completely degenerated by this stage. The endothelial cell layers eventually disrupted to release the mature pollen grains.

In the early premeiosis stage, there were no differences between wild-type anthers and *udt1-1* anthers. In *udt1-1* anthers, normal epidermis, endothecium, and secondary parietal cells were observed (Figures 6A, 6G, 6M, and 6S), and secondary parietal cells differentiated into middle layer and tapetum before meiosis (Figures 6M and 6S). During meiosis, *udt1-1* tapetal cells were continuously vacuolated (Figures 6N and 6T). However, the middle layers maintained their initial shape. At the tetrad stage, the tapetal cells of the *udt1-1* anther were further vacuolated and the dyads did not develop into tetrads (Figures 6O and 6U; see Supplemental Figure 1 online). To check for problems in the meiotic process, we performed 4',6-diamidino-2-phenylindole

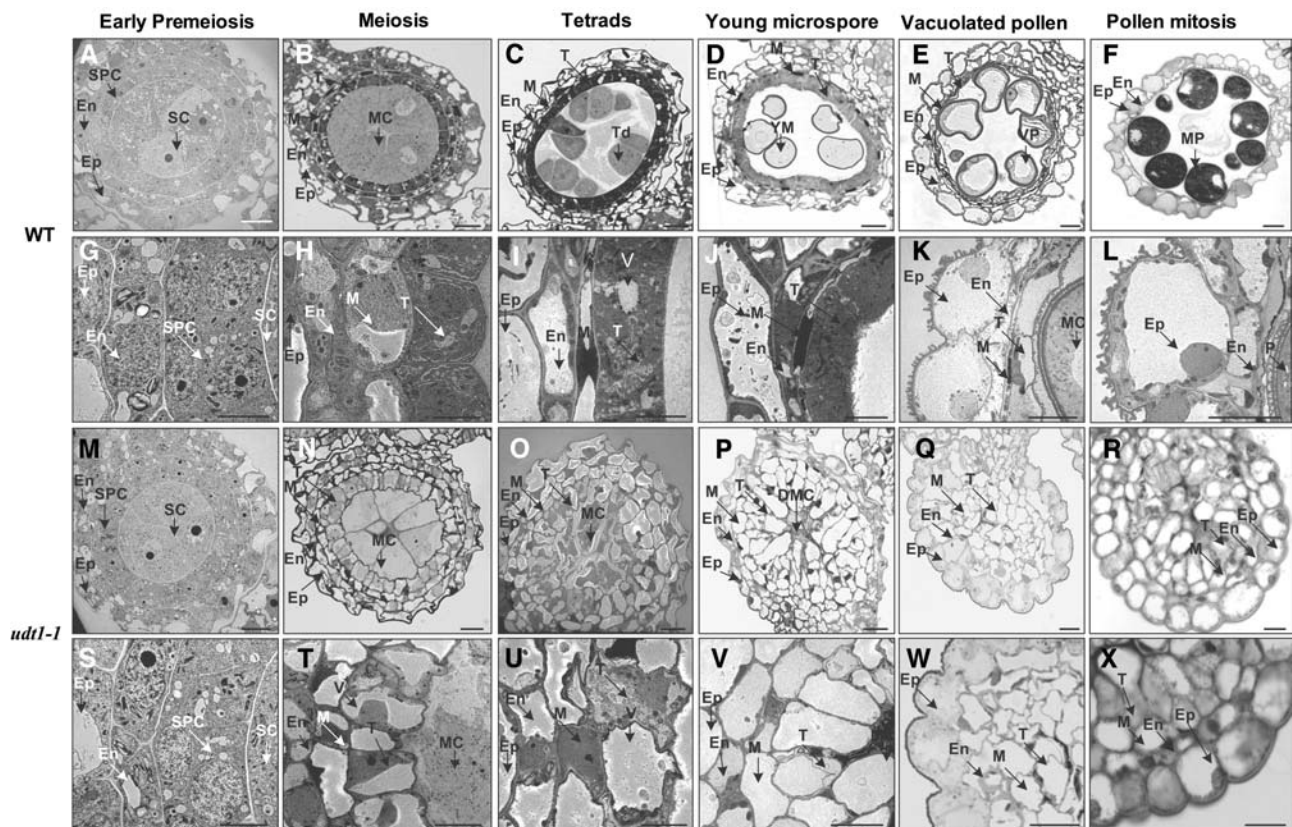


Figure 6. Transmission Electron Microscopy Analyses of Anthers in the Wild Type and *udt1* Mutants.

Cross sections of wild-type ([A] to [L]) and *udt1-1* ([M] to [X]) anthers at the early premeiotic stage ([A], [G], [M], and [S]), meiosis stage ([B], [H], [N], and [T]), tetrad stage ([C], [I], [O], and [U]), young microspore stage ([D], [J], [P], and [V]), vacuolated pollen stage ([E], [K], [Q], and [W]), and pollen mitosis stage ([F] and [L]). ([R] and [X] show cross sections of *udt1-2* anthers at the young microspore stage. DMC, degenerated meiocyte; En, endothelial cell layer; Ep, epidermal cell layer; M, middle layer; MC, meiocyte; MP, mature pollen; SC, sporogenous cell; SPC, secondary parietal cell; T, tapetal cell layer; Td, tetrad; V, vacuole; VP, vacuolated pollen; YM, young microspore. Bars = 10 μ m in (A) to (F) and (M) to (R) and 5 μ m in (G) to (L) and (S) to (X).

(DAPI) staining for wild-type and *udt1-1* anthers at meiosis to tetrads. We determined that *udt1-1* meiocytes underwent normal meiotic cell division like wild-type meiocytes but that they were degenerated at tetrads. We also found that the DAPI staining pattern in *udt1-1* was different from that in the wild type: the wild type showed overall strong DAPI staining in the tapetum, but DAPI staining in the *udt1-1* tapetum was preferential in the nuclei (see Supplemental Figure 2 online). In the young microspore and vacuolated pollen stages, the *udt1-1* meiocytes were completely degenerated, leaving only their remnants at the center of the anther locules, whereas the tapetum became abnormally large and extremely vacuolated (Figures 6P, 6Q, 6V, and 6W). At the pollen mitosis stage, the tapetal cells ruptured, thereby emptying the anthers (data not shown). At the young microspore stage, the cross section of the *udt1-2* anther also showed the same mutant phenotypes as those of *udt1-1* (Figures 6R and 6X). These observations suggest that UDT1 begins to function at the meiosis stage for tapetum development and pollen mother cell meiosis. Moreover, this gene is needed to degenerate the middle layer.

UDT1 Is Required for Early Tapetum Development and Pollen Mother Cell Meiosis

To investigate the functional roles of UDT1 in tapetum development, we studied the expression levels of rice tapetal marker genes (*Osc4*, *Osc6*, and *Cys protease1* [*Cp1*]) in the *udt1-1* and wild-type anthers (Figure 7). These genes are expressed preferentially in the tapetum and are involved in the development or degeneration of tapetal cells (Tsuchiya et al., 1994; Lee et al., 2004). Our analyses of the wild-type anthers show that the genes

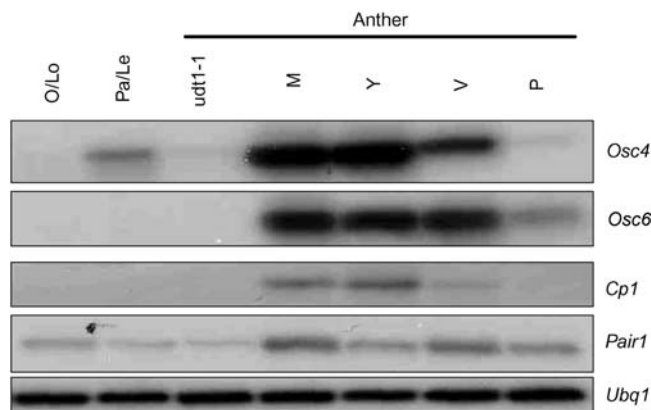


Figure 7. RT-PCR Analyses of Expression Levels for the Tapetal Marker Genes *Osc4*, *Osc6*, and *Cp1* and the Meiosis-Related Gene *Pair1*.

Primers were located on different exons; therefore, PCR products of cDNA were shorter than the genomic DNA product. PCR products were separated on an agarose gel, blotted onto a membrane, and hybridized with gene-specific probes. Samples were from ovaries/locules and paleas/lemmas of wild-type spikelets and from *udt1-1* anthers. Samples were also prepared from wild-type anthers at meiosis to the pollen mitosis stages. *Ubq1* was used as a control. Results from one representative experiment of at least three replicates are shown. O, ovary; Lo, lodicule; Pa, palea; Le, lemma; M, meiosis; Y, young microspore; V, vacuolated pollen; P, pollen mitosis.

were expressed at early stages and that transcript levels were reduced as the anther developed into the vacuolated and pollen mitosis stages. In the *udt1-1* anthers, however, transcripts for those marker genes were undetectable, suggesting that they are downstream of *Udt1*. These results indicate that tapetal function in the *udt1* mutant is severely disrupted at the early developmental stages.

We also studied the expression pattern of rice *Pair1* (for *homologous pairing aberration in rice meiosis1*), which is highly expressed in meiocytes and controls meiotic division (Nonomura et al., 2004a). Our analysis showed that its transcript was reduced to a low level in the *udt1-1* anthers, indicating that the development of meiocytes could be affected by the mutation (Figure 7).

Transcriptome Analyses of Wild-Type and *udt1-1* Anthers

We compared genome-wide mRNA levels of the wild-type and *udt1-1* anthers by microarray analyses of the 60,727-oligonucleotide DNA chip. Total RNAs were prepared from both anther sources at the meiosis/young microspore stages. The wild-type cDNA was labeled with Cy3, whereas the *udt1* cDNA was labeled with Cy5. To assess the reproducibility of the signals, the experiment was repeated by dye swapping. We also repeated the analysis with another set of anthers from the wild type and the mutant.

These analyses identified 958 genes that had at least twofold higher expression in the *udt1-1* anthers than in the wild-type anthers. Another 267 genes were found to have at least twofold lower expression in the mutant anthers (Table 1; see Supplemental Table 1 online). Putative functions were obtained from the Knowledge-Based Oryza Molecular Biological Encyclopedia (<http://cdna01.dna.affrc.go.jp/cDNA/>), The Institute for Genomic Research (<http://tigrblast.tigr.org/euk-blast/>), GAAS (<http://ricegaas.dna.affrc.go.jp/>), NCBI (<http://www.ncbi.nlm.nih.gov/>), and Clusters of Orthologous Groups (COG; <http://www.ncbi.nlm.nih.gov/COG/>) databases.

All 1225 genes mentioned above were then classified according to their functioning via COG analysis (Table 2). Major upregulated or downregulated genes in the *udt1-1* anthers included those involved in signal transduction and posttranslational modification/protein turnover/chaperones. Genes active in transcriptional regulation, intracellular trafficking/secretion/vesicular transport, translation/ribosomal structure/biogenesis, defense mechanisms, and lipid transport/metabolism were more numerous in the downregulated genes, whereas those involved in amino acid transport/metabolism and cell wall/membrane/envelope biogenesis were relatively more numerous in the upregulated group.

To investigate sequential expression patterns during anther development, we performed additional microarray analyses, comparing paleas/lemmas with anthers at four different stages: meiosis, young microspore, vacuolated pollen, and pollen mitosis (Figure 8; see Supplemental Table 1 online). The experiment was repeated by dye swapping. Consistent relationships between a microarray set and its dye-swap counterpart show that the microarray experiments are reliable (see Supplemental Figure 3 online).

To verify these microarray data, we selected six genes that were at least twofold downregulated and two that were at

Table 1. Partial List of the Genes That Are Upregulated or Downregulated at Least Twofold in *udt1-1* Anthers

CHR_Locus	udt1-1	M	Y	V	P	Putative Function	Group ^a
Carbohydrate transport/metabolism							
Os04g48400	-5.240 ± 0.428	4.519 ± 0.097	5.503 ± 0.570	4.011	0.590	GMC oxidoreductase	III
Os01g12030	-3.055 ± 1.010	2.118 ± 0.304	3.196 ± 0.523	1.193 ± 1.924	0.241 ± 1.532	Glycosyl hydrolase	II
Os09g20510	-3.609 ± 0.464	2.576 ± 0.136	1.852 ± 0.666	-0.380 ± 0.623	-0.522 ± 0.735	Sugar transporter	II
Os03g10090	-3.031 ± 1.071	1.096 ± 0.028	0.760 ± 1.912	-0.556 ± 0.870	-1.157 ± 0.636	Sugar transporter	II
Os08g08070	-2.970 ± 0.252	1.564 ± 0.254	0.701 ± 1.260	-0.300 ± 0.598	0.048 ± 0.541	Sugar transporter	II
Os01g38670	-1.918 ± 0.349	1.113 ± 0.322	3.329 ± 0.946	2.227 ± 1.291	-0.699	Sugar transporter	III
Cell cycle control/cell division/chromosome partitioning							
Os03g42070	-2.524 ± 0.390	1.495 ± 0.343	0.465 ± 0.611	-0.650 ± 0.724	-0.913 ± 0.366	G1/S-specific cyclin D	I
Os06g41710	-3.635 ± 1.175	3.195 ± 0.264	0.000	2.368	0.000	MORC family ATPases	I
Os12g43120	-2.572 ± 1.774	1.062 ± 0.119	1.358 ± 1.938	-0.543 ± 0.430	-0.497 ± 0.056	Anaphase-promoting complex	II
Cell wall/membrane/envelope biogenesis							
Os01g60770	1.233 ± 0.634	0.068 ± 0.206	0.069 ± 0.777	0.571 ± 0.313	0.013 ± 1.168	Expansin	V
Os03g01610	2.336 ± 0.130	-0.833 ± 0.095	-0.327	0.233	-0.007 ± 0.365	Expansin (pollen allergen)	V
Intracellular trafficking/secretion/vesicular transport							
Os12g35360	-2.188 ± 1.122	1.110 ± 0.295	2.853 ± 1.671	3.207 ± 1.557	2.114 ± 0.067	Endoplasmic reticulum–Golgi vesicle protein	III
Os06g16280	-2.115 ± 1.788	1.448 ± 0.052	2.787 ± 1.547	2.886 ± 1.964	2.133 ± 0.096	Predicted importin 9	III
Os07g48220	-2.867 ± 2.190	0.714 ± 0.471	1.313 ± 1.763	1.286 ± 1.858	1.645 ± 1.194	Vacuolar sorting receptor	III
Os01g49440	-1.923 ± 1.810	0.287 ± 0.315	0.900 ± 0.310	0.663 ± 0.086	0.431 ± 0.900	Synaptic vesicle	III
Os08g06470	-1.659 ± 0.753	0.624 ± 0.184	0.223 ± 0.479	-0.680 ± 0.316	-0.420 ± 0.287	Endosomal proteins	III
Os02g56110	-1.311 ± 0.375	0.648 ± 0.001	0.654 ± 0.193	0.313 ± 0.166	0.350 ± 0.172	Vesicle coat complex AP-1	III
Lipid transport/metabolism							
Os03g07140	-3.484 ± 0.846	3.055 ± 1.344	2.870 ± 0.375	1.180 ± 1.765	0.672	Acyl-CoA reductase (AtMS2)	II
Os08g20200	-2.761 ± 1.004	2.181 ± 0.718	3.544 ± 2.1651	0.937 ± 0.418	-0.684 ± 0.840	Acyl-CoA reductase	II
Os02g01980	-3.848 ± 0.234	2.410 ± 0.330	2.107 ± 0.503	0.310 ± 0.599	-0.506 ± 0.012	Lipase	II
Os09g39410	-2.484 ± 1.240	2.689 ± 0.938	4.116 ± 0.483	3.537 ± 0.596	2.743 ± 1.395	Acyl-CoA reductase (AtMS2)	III
Os08g44360	-3.209 ± 1.053	1.827 ± 0.225	2.575 ± 0.443	1.344 ± 0.036	0.294 ± 0.339	Acyl-CoA reductase (AtMS2)	III
Posttranslational modification/protein turnover/chaperones							
Os09g27940	-3.930 ± 0.388	2.842 ± 0.679	2.124 ± 0.514	-0.982 ± 1.731	-1.575 ± 0.289	Aspartyl protease	II
Os01g50170	-3.727 ± 0.325	2.114 ± 0.551	1.190 ± 1.900	-0.279 ± 1.109	-0.730 ± 0.331	Aspartyl protease	II
Os03g08790	-1.907 ± 0.384	1.531 ± 0.109	1.732 ± 0.272	0.308 ± 0.291	-0.136 ± 0.993	Aspartyl protease	II
Os11g10910	-2.450 ± 0.936	2.171 ± 0.108	2.296 ± 0.185	0.947 ± 0.473	0.926 ± 1.650	Aspartyl protease	II
Os07g49150	1.425 ± 0.171	-0.541 ± 0.044	0.260 ± 0.891	0.978 ± 0.506	0.061 ± 0.110	26S proteasome complex	IV
Os01g24550	2.778 ± 1.442	0.119 ± 0.227	1.287	3.512 ± 2.900	2.516 ± 0.781	Cys protease	IV
Os09g21370	4.676 ± 0.542	-0.095 ± 0.127	4.056 ± 1.162	5.359 ± 1.607	5.718 ± 0.101	Cys protease	IV
Os04g45960	-4.986 ± 1.621	4.147 ± 0.586	4.401 ± 0.405	2.647	-0.206 ± 0.859	Ser protease	II
Os05g30580	-1.352 ± 0.025	0.774 ± 0.277	0.375 ± 0.344	-0.147 ± 0.106	0.110 ± 0.304	Ser protease	II
Os03g40830	-4.109 ± 2.747	2.307 ± 0.410	2.343 ± 1.075	0.409 ± 0.887	-0.019 ± 0.775	Ser protease	II
Os08g43290	-3.226 ± 1.513	1.559 ± 0.449	2.034 ± 0.295	0.702 ± 2.742	-0.687 ± 2.807	Ser protease inhibitor	II
Os11g37280	-3.104 ± 2.072	1.522 ± 0.817	2.474 ± 0.159	1.730 ± 0.490	0.432 ± 0.927	Ser protease inhibitor	III
Secondary metabolites/biosynthesis/transport/metabolism							
Os07g31770	-3.941 ± 1.868	2.445 ± 0.727	2.026 ± 0.303	-1.005 ± 0.416	-0.977 ± 0.537	Chalcone synthase	II
Os11g18570	1.969 ± 2.751	-2.558 ± 0.244	-2.991 ± 1.180	-2.799 ± 0.585	-2.518 ± 0.679	Cytochrome P450	V
Signal transduction mechanisms							
Os10g02990	-4.585	4.825 ± 0.655	3.585	2.545	0.000	LRR receptor–like kinase	III
Os09g30190	-3.839 ± 0.525	2.314 ± 0.340	3.075 ± 0.933	-0.859 ± 2.990	-1.805	LRR receptor–like kinase	II
Os02g02490	-1.834 ± 0.629	0.977 ± 0.215	0.854 ± 1.118	0.295 ± 0.072	0.496 ± 0.640	LRR receptor–like kinase	III
Os04g57630	-2.456 ± 1.071	1.034 ± 0.432	2.367 ± 0.402	1.164 ± 0.450	0.072 ± 0.756	LRR receptor–like kinase	III
Transcriptional regulation							
Os02g46560	-5.117 ± 2.777	2.165 ± 0.0480	0.449 ± 0.268	0.823 ± 1.134	-1.874 ± 1.194	bHLH transcription factor	I
Os06g33450	-3.218 ± 0.732	1.846 ± 0.281	1.389 ± 1.009	-0.181 ± 0.018	0.579	bHLH transcription factor	II
Os01g72370	-2.032 ± 0.551	1.400 ± 0.143	1.095 ± 0.615	0.010 ± 0.644	0.508 ± 0.689	bHLH transcription factor	III
Os11g25560	-2.639 ± 0.299	0.546 ± 0.350	3.079 ± 0.951	4.158 ± 3.094	1.908 ± 0.470	bHLH transcription factor	III

(Continued)

Table 1. (continued).

CHR_Locus	udt1-1	M	Y	V	P	Putative Function	Group ^a
Os01g39330	-2.741 ± 0.939	1.620 ± 0.119	1.153 ± 1.670	0.108 ± 0.078	-0.036 ± 0.673	bHLH transcription factor	II
Os06g49040	-2.439 ± 1.391	0.967 ± 0.332	3.191 ± 1.363	3.242 ± 1.549	2.569 ± 0.104	MYB transcription factor	III
Os04g39470	-5.132 ± 2.257	3.328 ± 1.074	1.601 ± 1.461	-0.270	0.000	MYB transcription factor	I
Os01g03720	-.0505 ± 0.0405	1.084 ± 0.229	0.637 ± 1.199	0.225 ± 0.168	0.054 ± 0.371	MYB transcription factor	II
Os05g49310	-2.590 ± 0.332	2.741 ± 0.567	2.545 ± 1.406	0.123 ± 0.721	0.495 ± 1.178	MYB transcription factor	II
Os05g40960	-1.316 ± 0.674	0.222 ± 0.320	-0.010 ± 0.341	-0.560 ± 0.060	-0.622 ± 0.406	MYB transcription factor	II
Os02g07170	-2.232 ± 0.318	1.646 ± 0.205	0.768 ± 0.923	0.017 ± 0.513	0.185 ± 0.960	MYB transcription factor	I
Os07g40570	-2.478 ± 1.442	1.222 ± 0.096	0.939 ± 0.330	0.922 ± 0.108	0.774 ± 0.171	WRKY transcription factor	III
Os06g30860	-2.976 ± 0.898	1.967 ± 0.409	1.788 ± 0.783	0.028 ± 0.201	-0.305 ± 0.821	WRKY transcription factor	II
Os01g47560	-3.199 ± 0.872	1.818 ± 0.0061	1.738 ± 1.305	0.249 ± 0.225	-0.287 ± 0.575	WRKY transcription factor	II
Os01g40430	-4.604 ± 4.090	0.912 ± 0.502	0.272 ± 0.327	-0.290 ± 0.522	-0.034 ± 0.061	WRKY transcription factor	II
Os02g26430	-1.563 ± 1.547	-0.113 ± 0.597	-0.443 ± 1.931	-0.932 ± 0.513	-0.354 ± 1.479	WRKY transcription factor	III
Translation/ribosomal structure/biogenesis							
Os11g04070	-1.701 ± 1.184	0.684 ± 0.334	1.275 ± 1.053	1.222 ± 0.797	-0.059 ± 0.402	60S ribosomal protein P0	III
Os11g04070	-1.948 ± 0.988	0.605 ± 0.096	1.494 ± 0.504	0.829 ± 0.096	0.524 ± 0.761	60S ribosomal protein P0	III
Os12g03880	-2.160 ± 1.832	0.634 ± 0.173	0.469 ± 0.1146	3.061 ± 3.763	0.178 ± 0.596	60S ribosomal protein P0	III
Os10g32820	-1.653 ± 0.921	0.526 ± 0.062	1.202 ± 0.612	0.806 ± 0.114	-0.140 ± 0.692	60S ribosomal protein L21	III

CHR_locus (http://www.tigr.org/tdb/e2k1/osa1/tigr_gene_nomenclature.shtml) is the chromosomal locus of genes that are upregulated or downregulated at least twofold in the *udt1-1* anthers during meiosis to the young microspore stages. The genes not represented in Table 1 are listed in Supplemental Table 1 online. Log ratios with base 2 for the *udt1-1*/wild-type anthers at meiosis to the young microspore stages (*udt1-1*) are average values from three replicate experiments. Log ratios with base 2 for meiosis stage anthers/paleas/lemmas (M), young microspore stage/paleas/lemmas (Y), vacuolated pollen stage/paleas/lemmas (V), and pollen mitosis stage/paleas/lemmas (P) are average values from two replicate experiments. Genes are grouped based on their predicted functions; those confirmed by RT-PCR are shown in boldface. Tapetal marker genes are underlined. LRR, leucine-rich repeat; GMC, glucose-methanol-choline.

^a Groups were classified by hierarchical clustering in Figure 8.

least twofold upregulated in the *udt1-1* anthers (Os numbers in boldface type in Table 1). RT-PCR analyses were then performed on these genes (Figure 9). The downregulated genes, Os02g46560 (bHLH), Os04g39470 (MYB), Os03g07140 (OsMS2), Os04g45960 (Ser protease), Os04g48400 (oxidoreductase), and Os01g12030 (glycosyl hydrolase), were strongly expressed during the meiosis and young microspore stages but were severely repressed in the *udt1-1* anthers. The RT-PCR data were similar to those obtained from the microarray analyses. Of the selected upregulated genes, Os09g21370 (Cys protease) showed weak expression at the meiosis and young microspore stages, but levels increased as the anthers developed further to the vacuolated pollen and pollen mitosis stages. By contrast, Os11g18570 (cytochrome P450) was weakly expressed in the anthers. However, transcript levels of both genes were increased in the *udt1-1* anthers, as had also been observed with our microarray data.

We also checked to determine whether the tapetal marker genes (Figure 7) had been identified via microarray analyses. In fact, two of the genes (*Osc4* and *Osc6*) were downregulated in the *udt1* mutant anthers (Table 1, underlined). However, two others (*Cp1* and *Pair1*) were not included in the microarray data, probably because of the degree of their expression. Transcript levels were very low and only weakly detectable after 38 PCR cycles. These results indicate that weakly expressed genes are not distinguishable or detectable in the oligochip microarray analysis.

Hierarchical clustering of the 1225 genes (Figure 8) showed that the downregulated genes could be classified into three groups. Group I (157 genes) showed strong expression in the

anthers during meiosis (Figure 8, I). Group II genes (402 genes) were strongly expressed during meiosis and at the young microspore stage (Figure 8, II), whereas those in group III (299 genes) showed strong expression during the young microspore and vacuolated pollen stages (Figure 8, III). By contrast, the upregulated genes could be divided into two groups: group IV (82 genes) having strong expression after the vacuolated pollen stage (Figure 8, IV), but with most belonging to group V (185 genes), in which expression was relatively weak in the anthers (Figure 8, V).

Group I includes two putative transcription factor genes (Figure 9): Os02g46560 (bHLH) and Os04g39470 (MYB). Although the former is highly similar to *Arabidopsis* bHLH096, its function, as related to tapetum development, has not yet been reported. Its promoter region possesses two E-box (CANNTG) elements that are potential MYC recognition sites. Os04g39470 (MYB), similar to *Arabidopsis* MYB103, is expressed in the tapetum of developing anthers; its underexpression causes defects during pollen, tapetum, and trichome development (Higginson et al., 2003). The promoter region of this rice MYB gene contains four E-box elements. In addition to these two genes, six transcription factors were identified in this group: MYB (Os02g07170), GATA (Os11g04720), two zinc finger transcription factors (Os12g18120 and Os12g10660), and two heat shock transcription factors (Os03g53340 and Os08g36700). We speculate that these play major roles in controlling the early stages of anther development.

Finally, group I also includes genes related to cell cycle control, cell division, chromosome partitioning, and chromatin

Table 2. Functional Classification by COG Analysis of Genes That Are Upregulated or Downregulated at Least Twofold in the *udt1-1* Anthers

Function	Down	I	II	III	Up	VI	V	Total
Information storage and processing								
Translation/ribosomal structure/biogenesis	14	0	3	11	2	0	2	16
RNA processing/modification	14	2	5	7	4	2	2	18
Transcriptional regulation	62	10	31	21	6	1	5	68
Replication/recombination/repair	12	3	4	5	3	0	3	15
Chromatin structure/dynamics	5	2	0	3	0	0	0	5
Cellular processing and signaling								
Cell cycle/cell division/chromosome partitioning	8	5	3	0	2	0	2	10
Defense mechanisms	20	0	13	7	5	3	2	25
Signal transduction mechanisms	52	6	23	23	19	6	13	71
Cell wall/membrane/envelope biogenesis	9	1	3	5	7	0	7	16
Cytoskeleton	4	3	0	1	2	1	1	6
Extracellular structure	0	0	0	0	1	1	0	1
Intracellular trafficking/secretion/vesicular transport	12	1	3	8	1	0	1	13
Posttranslational modification/protein turnover/chaperones	67	10	36	21	21	8	13	98
Metabolism								
Energy production/conversion	12	2	4	6	4	0	4	16
Carbohydrate transport/metabolism	34	5	22	7	14	5	9	48
Amino acid transport/metabolism	11	4	5	2	8	3	5	19
Nucleotide transport/metabolism	5	3	2	0	0	0	0	5
Coenzyme transport/metabolism	0	0	0	0	1	1	0	1
Lipid transport/metabolism	41	3	20	18	5	1	4	46
Inorganic ion transport/metabolism	13	0	7	6	6	5	1	19
Secondary metabolites/biosynthesis/transport/metabolism	26	8	11	7	10	3	7	36
Poorly characterized								
General function prediction only	68	15	32	21	27	9	18	89
Hypothetical protein	469	78	273	118	119	34	85	588
Total	958	157	402	299	267	82	185	1225

COGs (<http://www.ncbi.nlm.nih.gov/COG/old/>) were delineated by comparing protein sequences encoded in 43 complete genomes. I, II, III, IV, and V are groups I to V in Figure 8.

structure/dynamics. Os03g42070 is a putative G1/S-specific cyclin D1 gene that is critical for entry into, continuation of, and exit from the cell division cycle (Koroleva et al., 2004; Guo et al., 2005). Os06g41710 is highly similar to MORC ATPase family genes, which serve biological functions in both the meiotic and mitotic cells of multicellular organisms (Inoue et al., 1999) (Table 1; see Supplemental Table 1 online).

Group II, the largest, was expected to have important roles during early tapetum development. It includes genes related to carbon and lipid metabolism/transport, such as the three putative sugar transporters Os09g20510, Os03g10090, and Os08g08070 (Table 1). All three are probably involved in the uptake of sugar necessary for early development and pollen maturation (Truernit et al., 1999). Two genes (Os03g07140 and Os08g20200) that encode putative acyl-CoA reductase also belong to this group. The former shares high identity with *Arabidopsis* MS2, which is expressed during early tapetum development, thereby resulting in male sterility (Aarts et al., 1997). Anthers at the early developmental stages require a large amount of energy for tapetum differentiation and nursing of the developing pollen (Liu and Dickinson, 1989). Group II also includes 31 genes involved in transcriptional regulation, the

most notable being three WRKY, two bHLH, three MYB, and three APETALA2 transcription factor genes (see Supplemental Table 1 online). Together with the group I transcription factors, these play a key regulatory function in early anther development.

The late-stage genes of group III are likely associated with tapetum and pollen differentiation. Four components of the 60S ribosomal proteins and a component of the 40S ribosomal proteins are in this group. Genes related to intracellular trafficking/secretion/vesicular transport are also abundant in group III (Tables 1 and 2).

Group IV is the smallest; its genes appear to be involved in tapetum degeneration. For example, two Cys protease genes (Os09g21370 and Os01g24550) belong to this group. Another member, Os07g49150 (Table 1), encodes a putative 26S proteasome AAA-ATPase that mediates targeted proteolysis (Vierstra, 2003).

Finally, the genes belonging to group V are probably repressed during normal anther development. In particular, seven cell wall/membrane/envelope biogenesis genes and two expansin genes (Os01g60770 and Os03g01610) are included in this group (Table 1).

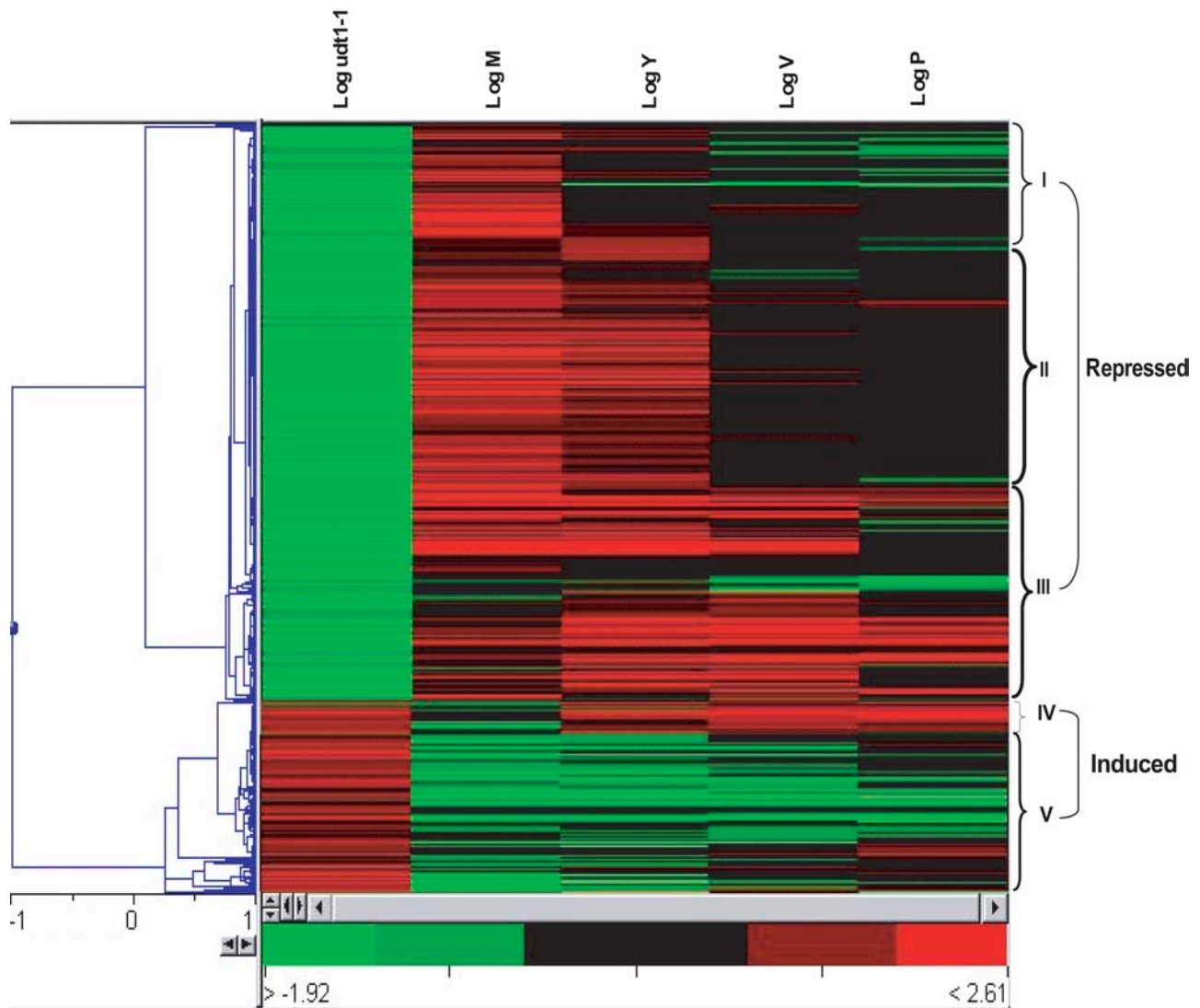


Figure 8. Hierarchical Clustering of 1225 Significant Spots That Were Upregulated or Downregulated at Least Twofold in *udt1-1* Anthers.

Microarray analyses of *udt1-1* and wild-type anthers at meiosis to young microspore stages were performed. To assess the reproducibility of the signals, the experiment was repeated with dye swapping and using two biological replicates. Genes that were upregulated or downregulated at least twofold were identified; their expression patterns during anther development were investigated by microarray analyses of palea/lemmas and anthers at meiosis (M), the young microspore stage (Y), vacuolated pollen stage (V), and pollen mitosis stage (P).

DISCUSSION

UDT1 Is a Major Regulator of Early Anther Development

We have identified male-sterile rice mutants that result from T-DNA or *Tos17* insertions into a putative bHLH transcription factor gene. At the premeiosis stage, the development of primary sporogenous cells and the four layers of the anther wall are normal in the *udt1* mutants. However, during meiosis, the tapetal layers in the mutant anthers begin to manifest premature degeneration as the vacuoles enlarge. In the wild type, tapetal cells are condensed and barriers among them are depleted. At later stages, the vacuolated cells of the *udt1-1* anthers enlarge and,

eventually, collapse. These results suggest that UDT1 plays a major role in maintaining tapetum development, starting at the early meiosis stage.

Our *udt1-1* flowers show other anther defects. For example, whereas the middle layer cells are degenerated in the wild-type anthers, this process does not occur in the mutants. In addition, their dyads do not develop into tetrads. The *udt1-1* meiocytes also suffer from severe contractions and possess many small vacuoles during late meiosis. Consequently, only the remnant of meiocytes remains in the mutant locules. These direct pleiotropic effects are probably attributable to the lack of *Udt1* gene functioning, because transcript is preferentially present in all cell types within the early anthers.

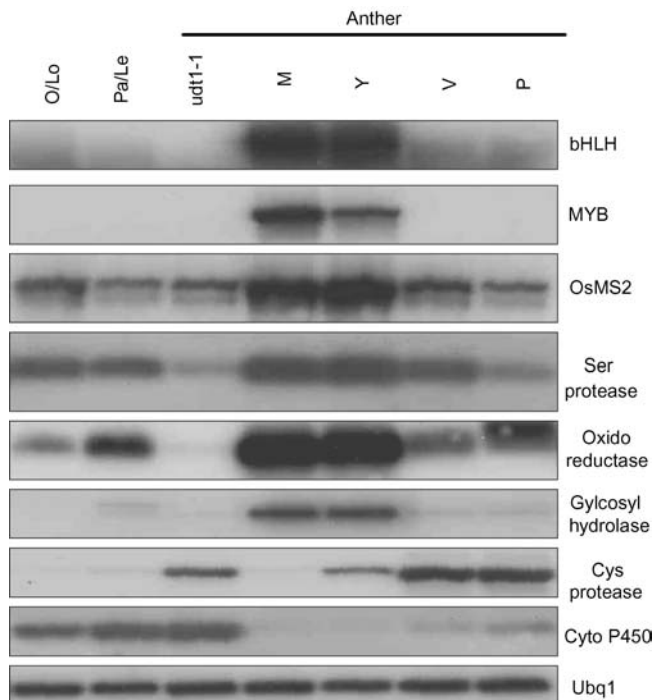


Figure 9. RT-PCR Analyses of Eight Genes Identified from Microarray Analyses.

Primers were located on different exons; therefore, PCR products of cDNA were shorter than the genomic DNA product. PCR products were separated on an agarose gel, blotted onto a membrane, and hybridized with gene-specific probes. RNA samples were prepared from ovaries/ lodicules and paleas/lemmas of wild-type spikelets and *udt1-1* anthers. Samples were also prepared from wild-type anthers at meiosis to the pollen mitosis stage. *Ubq1* was used as a control. Results from one representative experiment of at least three replicates are shown. O, ovary; Lo, lodicule; Pa, palea; Le, lemma; M, meiosis; Y, young microspore; V, vacuolated pollen; P, pollen mitosis; bHLH, Os02g46560; MYB, Os04g39470; OsMS2, Os03g07140; Ser protease, Os04g45960; oxidoreductase, Os04g48400; glycosyl hydrolase, Os01g12030; Cys protease, Os09g21370; Cyto P450, Os11g18570.

To demonstrate at the molecular level that the *udt1* mutations alter early tapetum development, we examined transcript levels for three early tapetal marker genes, *Cp1*, *Osc4*, and *Osc6* (Tsuchiya et al., 1994; Lee et al., 2004). These genes are expressed in wild-type anthers during early development. Their levels were severely reduced in our *udt1* mutant anthers, indicating that UDT1 regulates their expression. Furthermore, because proper meiosis did not occur in the mutants, we also examined the activity of the meiosis-related gene *Pair1* (Nonomura et al., 2004a). *Pair1* transcript was also reduced significantly in these mutant anthers, supporting at the molecular level the notion that meicyte development is regulated by UDT1.

***Udt1* Is Expressed Preferentially in Anthers at Early Developmental Stages**

The *Udt1* gene is preferentially expressed in the developing panicles, especially in the anthers. During the early stages, the

tapetal cells have the highest degree of transcriptional activity among all anther cell types (Raghavan, 1981, 1989; Kapoor et al., 2002). This gene is also expressed in both the anther wall and the meiocytes. However, expression levels are lower at later stages, suggesting that *Udt1* is involved not only in the initiation of cellular differentiation but also in maintaining anther formation. This gene is also weakly expressed in the vegetative tissues, although its role is unclear because our mutants showed no visible phenotype. Other genes, perhaps, compensate for this *udt1* mutation in those tissues.

The UDT1 Protein Is a Member of the Family of bHLH Transcription Factors

Because the *Udt1* gene product is a nuclear protein with a conserved bHLH motif, the UDT1 protein is likely a transcription factor that controls a set of genes important for the differentiation of the tapetum and meiocytes as well as for the degeneration of the middle layer.

By comparing protein sequences, we found that UDT1 was highly similar to *Arabidopsis* AMS and ICE1, which belong to the group 9 bHLH protein family. These bHLH proteins belong to the MYC-related bHLH proteins (Bouchard et al., 1998; Chinnusamy et al., 2003; Sorensen et al., 2003). AMS plays a crucial role in tapetal cell formation and the postmeiotic transcriptional regulation of microspore development (Sorensen et al., 2003). At the protein sequence level, the rice protein Os02g02820 (Os9630.m00194) is the most similar to *Arabidopsis* AMS. Because tapetal cell condensation and microspore formation occur in the *ams* mutant anthers, we believe that its rice homolog should function downstream of *Udt1*. We observed that the former was strongly expressed in anthers during early tapetum development and that its expression level was reduced in the mutants (data not shown), which further supports the possibility that the gene acts downstream of *Udt1*.

In addition to the putative AMS homolog, microarray analyses identified five additional bHLH genes that are downregulated in the *udt1-1* anthers (Table 1). Because bHLH proteins form heterodimers (Fairchild et al., 2000; Baudry et al., 2004), it is possible that interaction between these bHLH proteins and UDT1 may produce a functional transcription unit.

The *ICE1* gene encodes a MYC-like bHLH transcriptional activator that binds specifically to the MYC recognition sequences in the *C-REPEAT BINDING FACTOR3* promoter. *ICE1* is expressed constitutively, and its overexpression improves freezing tolerance in transgenic plants (Chinnusamy et al., 2003). The rice genome contains two bHLH genes that are highly homologous with *ICE1*. However, their expression is not affected by the *udt1* mutation, indicating that they are not involved in anther development (data not shown).

Roles of Other Transcription Factors during Anther Development

Microarray analyses of the *udt1* mutant anthers identified 1225 genes that are either upregulated or downregulated. The most downregulated class comprised genes that encode for transcription factors. Most of these are expressed early and are

downregulated in the mutant anthers. This fact demonstrates that they play important regulatory roles at those stages. In addition to the six bHLH genes described above, MYB transcription factors also were abundant, probably functioning together with bHLH to control proper anther development. The formation of heterodimers between MYC-type bHLH and MYB proteins has been reported (Elomaa et al., 2003; Zimmermann et al., 2004). The *Udt1* promoter contains E-box elements, which are known binding sites in the bHLH–MYB transcription complex (Bouchard et al., 1998; Sorensen et al., 2002; Abe et al., 2003; Chinnusamy et al., 2003). In particular, Os04g39470 was 95.2% similar to *Arabidopsis* Myb103, the underexpression of which causes defects in tapeta and young microspores. A pattern of strong expression at meiosis and the young microspore stage was also well matched with these developmental defects. Therefore, Os04g39470 could be involved in regulating early anther and tapetum development under the control of UDT1.

Our array analysis also identified five WRKY transcription factor genes whose expression patterns are similar to those of bHLH and MYB. They were most strongly expressed during the early stages; their expression was downregulated in the mutant anthers. The WRKY genes are also involved in disease resistance and stress responses (Eulgem et al., 2000; Kim and Zhang, 2004). Furthermore, Johnson et al. (2002) found that TRANSPARENT TESTA GLABRA2, another WRKY protein, functions in trichome development. The WRKY protein acts downstream of GLABROUS1, a MYB protein (Zhang et al., 2003). Therefore, it seems that WRKY has diverse functions.

Sun et al. (2003) have shown that a barley (*Hordeum vulgare*) WRKY transcription factor, SUGAR SIGNALING IN BARLEY2, participates in sugar signaling by binding to the sugar-responsive element (AATAGAAA). That element was present 1555 bp upstream from the start codon in one of the WRKY genes, Os06g30860, which we identified via microarray analyses. The promoter also contains another sugar-responsive element SPECIFICITY PROTEIN8 motif (TACTATT) at 706 bp upstream from the start codon (Ishiguro and Nakamura, 1994). From our transcriptome analysis, we also found genes (Os09g20510, Os03g10090, and Os08g08070; Table 1) that were strongly expressed in meiosis and at the young microspore stage and related to sugar metabolism, which plays important roles in the generation of microspores. Therefore, it is possible that the Os06g30860 protein is involved in sugar signaling under the transcriptional control of UDT1 during early anther development.

Roles of Other Genes during Anther Development

Expression levels of several protease genes were affected by the *udt1* mutation. Interestingly, most of the aspartyl protease and subtilin-like protease genes were downregulated and preferentially expressed during early tapetum development, whereas Cys proteases were primarily upregulated in *udt1-1* anthers and preferentially expressed later on. These observations demonstrate that the aspartyl protease and subtilin protease genes are important components of early anther development. Such proteases have broad functional roles, such as in plant development and disease resistance (Beers et al., 2004). In particular, the Cys

protease genes are associated with programmed cell death during various stresses and at senescence. Therefore, their likely function is in tapetum degeneration. Previously, two marker genes (*Osc4* and *Osc6*) that show tapetal preferential expression at early anther development and encode protease inhibitors were downregulated in *udt1-1* anthers. Another possible role of UDT1 may be to guide normal early anther development by maintaining the transcription of these two protease inhibitors via rice Myb103 (Os04g39470). The possible functions of UDT1 identified in the microarray analyses need confirmation by transcriptome analysis of *Udt1*-overexpressing anthers or by examining the genetic relationships of knockout mutants.

We first performed our array experiment using only *udt1-1* anthers at the mature anther stage; as a result, we found many genes that were preferentially or constitutively expressed in mature anthers (data not shown). In a subsequent microarray experiment using *udt1-1* anthers at meiosis and the young microspore stage, we were able to identify genes downstream of *Udt1* that were putatively involved in major phenotypic changes in the transition from tetrads to the young microspore stage. Although all of the listed genes were not downstream of *Udt1*, this analysis suggests that many genes may have important roles in early rice anther development. Among those expected to have significant roles in tapetum and early anther development are *Osc4* (Os08g43290), *Osc6* (Os11g37280), *OsMS2* (Os03g07140 and Os08g20200), *OsMyb103* (Os04g39470), *OsEMS1* (Os10g02990), and *Radc1* (Os03g08790) (Tsuchiya et al., 1994; Aarts et al., 1997; Canales et al., 2002; Zhao et al., 2002; Higginson et al., 2003; Yamaguchi et al., 2004). However, it is difficult to predict the functions of most of the significant genes because there have been few studies of early rice anther development. Earlier microarray experiments on rice anthers did not target early anther developmental stages at the whole genome level (Endo et al., 2004; Lan et al., 2004; Yamaguchi et al., 2004). Therefore, our microarray data should provide a good basis for the identification and analysis of the genes involved in early rice anther development.

METHODS

Plant Growth

Seeds of *udt1-1*, *udt1-2*, and wild-type rice (*Oryza sativa* cv Japonica) were germinated on Murashige and Skoog medium containing 0.44% Murashige and Skoog basal salt, 3% sucrose, 0.2% Phytigel, and 0.55 mM *myo*-inositol. The seedlings were grown for 1 week at 27°C under continuous light, then transplanted to soil in the greenhouse and raised to maturity.

Histochemical GUS Assays and Microscopic Analyses

Histochemical GUS staining was performed as described by Jefferson et al. (1987) and Dai et al. (1996), except for the addition of 20% methanol to the staining solution. For light microscopic analysis, the tissues were fixed in a solution containing 50% ethanol, 5% acetic acid, and 3.7% formaldehyde, then embedded in Paraplast (Sigma-Aldrich) and Technovit 8100 resin (Heraeus). The samples were sectioned to 3 to 16 μ m thickness with a microtome (Leica) and observed with a microscope (Nikon) using bright- and dark-field illumination.

Ultrastructural Analyses

Spikelets and anthers of the wild type and *udt1* mutant were sampled at various stages of development and fixed for 4 h in cacodylate buffer, pH 7.2, that contained 2% paraformaldehyde and 2% glutaraldehyde. They were then rinsed with the same buffer and postfixed for 1 h in cacodylate buffer containing 1% osmium tetroxide. After dehydration, the specimens were embedded in London Resin White (London Resin). Ultrathin sections (40 to 60 nm thick) collected on uncoated nickel grids (300 mesh) were stained with 4% uranyl acetate and examined at 60 to 80 kV with a JEOL 1200 transmission electron microscope.

RT-PCR and DNA Gel Blot Analyses

Total RNAs were isolated using Tri Reagent (Molecular Research Center). The mRNAs were acquired with a PolyATtract mRNA isolation system (Promega). For the first-strand cDNA synthesis, 200 ng of mRNA was reverse-transcribed in a total volume of 100 μ L that contained 10 ng of oligo(dT)₁₂₋₁₈ primer, 2.5 mM deoxynucleotide triphosphate (dNTP), and 200 units of Moloney murine leukemia virus reverse transcriptase (Promega) in a reaction buffer. PCR was performed in a 30- μ L solution containing a 1- μ L aliquot of the cDNA reaction, 0.2 μ M gene-specific primers, 10 mM dNTPs, 1 unit of ExTaq DNA polymerase (Takara), and reaction buffer. The reaction included an initial 5-min denaturation at 94°C, followed by 21 to 38 cycles of PCR (94°C for 45 min, 60°C for 45 min, and 72°C for 1 min), and a final 10 min at 72°C. Afterward, 10 μ L of the reaction mixture was separated on a 1.2% agarose gel, blotted onto a nylon membrane, and hybridized with ³²P-labeled gene-specific probes (see Supplemental Table 2 online) as described previously (Kang et al., 1998).

Isolation of T-DNA Flanking Sequence by TAIL-PCR

TAIL-PCR was performed as described previously (Liu et al., 1995). The template was cDNA prepared from the panicles of heterozygotic *udt1-1* plants collected at the vacuolated stage. The specific primers were *gus1* (5'-GCCGTAATGAGTGACCGCATCG-3'), *gus2* (5'-ATCTGCATCGGC-GAACTGATCG-3'), and *gus3* (5'-CACGGGTTGGGGTTTCTACAGG-3'). Arbitrary primers included ad1 [5'-NTCGA(G/C)T(G/C)G(A/T)GTT-3'], ad2 [5'-NGTCGA(G/C)(A/T)GANA(A/T)GAA-3'], and ad3 [5'-(A/T)GTGNAG-(A/T)ANCANAGA-3']. The third PCR product was subjected directly to sequencing using the *gus3* primer.

Genotyping the Mutant Plants and Isolating the Fusion Transcript between *Udt1* and *GUS*

All PCRs were performed in 50 μ L of a mixture containing 20 ng of plant DNA or 2 ng of cDNA, 10 \times ExTaq buffer, 0.2 mM dNTP, 0.5 unit of ExTaq polymerase, and 1 μ M of the primers. The protocol included 35 cycles of 94°C for 60 s, 60°C for 60 s, and 72°C for 90 s. Primers for genotyping were 5'-GATGGGAAGGAGTTCAAGT-3' (p1 in Figure 2A; 171 bp downstream from the ATG start codon of the *Udt1* gene), 5'-CATCACTTCCT-GATTATTGACC-3' (p2 in Figure 2A; 316 bp downstream from the ATG start codon of the *GUS* gene), and 5'-AGTTTATTGTAGTCAGGAGTG-3' (p3 in Figure 2A; 1581 bp downstream from the ATG start codon of the *Udt1* gene). We used p1 and p2 as primers to detect the fusion transcript between *Udt1* and *GUS*.

Screening the *Tos17* Insertional Allele in the *Udt1* Gene from DNA Pools

A *udt1* knockout line (*udt1-2*) was isolated by PCR screening of 20,000 insertional mutant lines with the *Udt1* gene-specific primers (5'-GTCAT-CAGTCATTCAGTCAAACATGTACC-3' and 5'-GCAATCTGGAAAATAT-GATCACTCAACTT-3') and the *Tos17* primers (5'-TCTCTATTGCTAA-

TACTATTGTTAGGTTGCAA-3' and 5'-GCTGGACATGGCCAACTATA-CAGTA-3'). The exact position of the *Tos17* insertion was determined by sequencing the amplified DNA fragment. All procedures were identical to those described by Lee et al. (2003). Briefly, the first round of PCR was conducted with template DNAs prepared from superpools of 1000 individuals. PCR products were then run on an agarose gel, blotted onto a nylon membrane, and hybridized with the gene-specific probe. The second- and third-round PCRs were conducted to identify an individual line that possessed a *Tos17* insertion in the *Udt1* gene.

In Vivo Targeting of GFP and RFP Fusion Constructs

Plasmid DNAs were purified on a Qiagen column according to the manufacturer's instructions. The fusion constructs were introduced into *Arabidopsis thaliana* protoplasts prepared from whole seedlings by the polyethylene glycol-mediated transformation procedure (Jin et al., 2001). Expression of the fusion constructs was monitored at various times after transformation by fluorescence microscopy (Zeiss Axioplan microscope), and the images were captured with a cooled charge-coupled device camera. The filter sets used were XF116 (Omega; exciter, 474AF20; dichroic, 500DRLP; emitter, 510AF23) for the GFP, XF33/E (exciter, 535DF35; dichroic, 570DRLP; emitter, 605DF50) for the RFP, and XF137 (exciter, 540AF30; dichroic, 570DRLP; emitter, 585ALP) for autofluorescence of the chlorophyll. The data were processed with Adobe Photoshop software and presented in a pseudocolor format. Primers for constructing the fusion vector were 5'-TGCTCTAGAAAAGTGCCATC-GAGTGTGGTT-3' (105 bp upstream from the ATG start codon of *Udt1*) and 5'-CGCGGATCCTTGGAACTCCACAATGCTG-3' (6 bp upstream from the TGA stop codon of *Udt1*).

60K Rice Whole Genome DNA Chip Analysis of the *udt1-1* and Wild-Type Anthers

Expression profiling was conducted with the 60K Rice Whole Genome Microarray (www.ggbio.com/rice60kchip.html; GreenGene Biotech). The 60K microarray was designed to represent all of the genes in rice. In total, 60,727 oligomers were designed from gene-specific regions of both *japonica* and *indica* subspecies. These include 58,417 from known and predicted genes and 66 randomized DNA oligomers. Among these, 2310 genes were also designed as antisense oligomers. Oligomer sequences were extracted by Qiagen-Operon based on rice genome information from the Beijing Genomics Institute. Oligomers were synthesized and purified by Qiagen-Operon and spotted on SuperAmine slides using the facilities of David Galbraith at the University of Arizona (<http://ag.arizona.edu/microarray/deconvolution.html>). A set of two slides of the 60K microarray has 64,896 spot addresses. Each slide is formatted with 48 (12 \times 4) blocks composed of 676 (26 \times 26) spot addresses. Blank spots (4099) were also included for easy scanning alignment. Each oligomer (70 nucleotides long and with an average T_m of 78°C) was printed in each spot address with a diameter of 100 μ m.

Three independent samples of total RNA (100 μ g) were prepared from *udt1-1* and wild-type anthers at meiosis to the young microspore stage, and the mRNA was purified from total RNA using the Qiagen oligotex column. To ascertain the sequential expression of each gene, we also prepared two samples of each of wild-type anthers at meiosis, young microspore stage, vacuolated pollen stage, and mature pollen stage and of paleas/lemmas at meiosis to the mature pollen stage. Developing anthers were classified according to flower length as referenced in Oryzabase (http://www.shigen.nig.ac.jp/rice/oryzabase/development/organAndStage.jsp;jsessionid=9C126A82E8659FC921692A861F35A431.tomcat4_6) and to panicle length (Hoshikawa, 1989) in the following categories: 2- to 4.5-mm flowers within 4- to 10-cm panicles, anthers at meiosis; 4.6- to 5.5-mm flowers within 11- to 15-cm panicles, young microspore stage; 5.6- to 7-mm flowers within 16- to 20-cm panicles,

vacuolated pollen stage; and 7-mm flowers within >22-cm panicles, mature pollen stage. Preparation of fluorescently labeled probes and microarray hybridization were performed according to procedures provided by the Genisphere 3 DNA array detection 50 kit (version 2). The microarray was scanned with Genepix 4000 B (Axon Instruments), and the quality of the chip data was analyzed with R statistical language and the *sma* package of the Bioconductor project (<http://www.bioconductor.org/>) implemented on a Linux platform. To assess the reproducibility of the microarray analysis, we repeated the experiment two or three times with independently prepared total RNA. A dye-swap test was also included to monitor the effect of the intrinsic intensity difference between Cy3 and Cy5. Noncorrelation of signal and background intensities was confirmed by plotting base 2 log background intensity on the x axis and base 2 log intensity subtracted from background intensity on the y axis. Before normalization, the normal distribution and linear relations of Cy3 and Cy5 intensities were tested by qqplot and a linear regression model, respectively, in R statistical language. The spatial effects on the chip during the hybridization process were checked with *spatial.func* in the *sma* package. The variance differences between Cy3 and Cy5 intensities within the microarray were tested with the *t* test under the assumption of both uniform and nonuniform variances. One- and two-way analyses of variance of the signal intensity differences between microarrays were performed. Median pixel intensities were transformed as log ratios with base 2 and then adjusted by block-by-block Lowess normalization for each slide (Yang et al., 2002). To improve the specificity of our statistical hypothesis in low-intensity regions, we adopted the following empirical criteria: a spot was selected if it was not flagged for its morphology, the diameter was larger than 51 pixels, and the intensities of both signals were higher than 500. Multivariate statistical tests such as clustering, principal component analysis, and multidimensional scaling were performed with Acuity 3.1 (Axon Instruments). All of our raw data can be retrieved from the NCBI Gene Expression Omnibus database (<http://www.ncbi.nlm.nih.gov/projects/geo/>; accession number GSE2619).

Accession Numbers

Sequence data for the mRNA and genomic DNA of *Udt1* can be found in the GenBank/EMBL data libraries under accession numbers AY953870 and AAX55226, respectively.

ACKNOWLEDGMENTS

This work was supported, in part, by grants from the Crop Functional Genomic Center, the 21st Century Frontier Program (Grant CG1111 to G.A. and Grant CG1411 to B.H.N.); from the Biogreen 21 program, Rural Development Administration (to G.A. and B.H.N.); and from the Pohang Iron and Steel Company (to G.A.). We thank Kyungsook An for screening the *Tos17* insertional mutant in the *Udt1* gene, Sung-Ryool Kim for DNA sequencing, In-Soon Park for generating transgenic plants, Jong-Seong Jeon for helpful discussion, Jongmin Nam for phylogenetic analysis, and Priscilla Licht for English editing.

Received May 6, 2005; revised July 6, 2005; accepted August 10, 2005; published September 2, 2005.

REFERENCES

- Aarts, M.G.M., Hodge, R., Kalantidis, K., Florack, D., Wilson, Z.A., Mulligan, B.J., Stiekema, W.J., Scott, R., and Pereira, A. (1997). The *Arabidopsis* MALE STERILITY 2 protein shares similarity with reductases in elongation/condensation complexes. *Plant J.* **12**, 615–623.
- Abe, H., Urao, T., Ito, T., Seki, M., Shinozaki, K., and Yamaguchi-Shinozaki, K. (2003). *Arabidopsis* AtMYC2 (bHLH) and AtMYB2 (MYB) function as transcriptional activators in abscisic acid signaling. *Plant Cell* **15**, 63–78.
- An, G., Lee, S., Kim, S.-H., and Kim, S.-R. (2005). Molecular genetics using T-DNA in rice. *Plant Cell Physiol.* **46**, 14–22.
- Armstrong, S.J., Caryl, A.P., Jones, G.H., and Franklin, F.C. (2002). Asy1, a protein required for meiotic chromosome synapsis, localizes to axis-associated chromatin in *Arabidopsis* and *Brassica*. *J. Cell Sci.* **115**, 3645–3655.
- Azumi, Y., Liu, D., Zhao, D., Li, W., Wang, G., Hu, Y., and Ma, H. (2002). Homolog interaction during meiotic prophase I in *Arabidopsis* requires the *SOLO DANCERS* gene encoding a novel cyclin-like protein. *EMBO J.* **21**, 3081–3095.
- Baudry, A., Heim, M.A., Dubreucq, B., Caboche, M., Weisshaar, B., and Lepiniec, L. (2004). TT2, TT8, and TTG1 synergistically specify the expression of BANYULS and proanthocyanidin biosynthesis in *Arabidopsis thaliana*. *Plant J.* **39**, 366–380.
- Beers, E.P., Jones, A.M., and Dickerman, A.W. (2004). The S8 serine, C1A cysteine and A1 aspartic protease families in *Arabidopsis*. *Phytochemistry* **65**, 43–58.
- Bouchard, C., Staller, P., and Eilers, M. (1998). Control of cell proliferation by Myc. *Trends Cell Biol.* **8**, 202–206.
- Canales, C., Bhatt, A.M., Scott, R., and Dickinson, H. (2002). EXS, a putative LRR receptor kinase, regulates male germline cell number and tapetal identity and promotes seed development in *Arabidopsis*. *Curr. Biol.* **12**, 1718–1727.
- Chaubal, R., Anderson, J.R., Trimmell, M.R., Fox, T.W., Albertsen, M.C., and Bedinger, P. (2003). The transformation of anthers in the *msca1* mutant of maize. *Planta* **216**, 778–788.
- Chaudhury, A. (1993). Nuclear genes controlling male fertility. *Plant Cell* **5**, 1277–1283.
- Chinnusamy, V., Ohta, M., Kanrar, S., Lee, B.-H., Hong, X., Agarwal, M., and Zhu, J.-K. (2003). ICE: A regulator of cold-induced transcriptome and freezing tolerance in *Arabidopsis*. *Genes Dev.* **17**, 1043–1054.
- Coller, H.A., Grandori, C., Tamayo, P., Colbert, T., Lander, E.S., Eisenman, R.N., and Golub, T.R. (2000). Expression analysis with oligonucleotide microarrays reveals that MYC regulates genes involved in growth, cell cycle, signaling, and adhesion. *Proc. Natl. Acad. Sci. USA* **97**, 3260–3265.
- Dai, Z., Gao, J., An, K., Lee, J.M., Edwards, G.E., and An, G. (1996). Promoter elements controlling developmental and environmental regulation of a tobacco ribosomal protein gene *L34*. *Plant Mol. Biol.* **32**, 1055–1065.
- Elomaa, P., Uimari, A., Mehto, M., Albert, V.A., Laitinen, R.A., and Teeri, T.H. (2003). Activation of anthocyanin biosynthesis in *Gerbera hybrida* (Asteraceae) suggests conserved protein-protein and protein-promoter interactions between the anciently diverged monocots and eudicots. *Plant Physiol.* **133**, 1831–1842.
- Endo, M., Tsuchiya, T., Saito, H., Matsubara, H., Hakozaiki, H., Masuko, H., Kamada, M., Higashitani, A., Takahashi, H., Fukuda, H., Demura, T., and Watanabe, M. (2004). Identification and molecular characterization of novel anther-specific genes in *Oryza sativa* L. by using cDNA microarray. *Genes Genet. Syst.* **79**, 213–226.
- Eulgem, T., Rushton, P.J., Robatzek, S., and Somssich, I.E. (2000). The WRKY superfamily of plant transcription factors. *Trends Plant Sci.* **5**, 199–206.
- Fairchild, C.D., Schumaker, M.A., and Quail, P.H. (2000). HFR1 encodes an atypical bHLH protein that acts in phytochrome A signal transduction. *Genes Dev.* **14**, 2377–2391.
- Glover, J., Grelon, M., Craig, S., Chaudhury, A., and Dennis, E.

- (1998). Cloning and characterization of *MS5* from *Arabidopsis*: A gene critical in male meiosis. *Plant J.* **15**, 345–356.
- Goldberg, R.B., Beals, T.P., and Sanders, P.M.** (1993). Anther development: Basic principles and practical applications. *Plant Cell* **5**, 1217–1229.
- Guo, Y., Harwalkar, J., Stacey, D.W., and Hitomi, M.** (2005). Destabilization of cyclin D1 message plays a critical role in cell cycle exit upon mitogen withdrawal. *Oncogene* **24**, 1032–1042.
- Higginson, T., Li, S.F., and Parish, R.W.** (2003). AtMYB103 regulates tapetum and trichome development in *Arabidopsis thaliana*. *Plant J.* **35**, 177–192.
- Hoshikawa, K.** (1989). *The Growing Rice Plant: An Anatomical Monograph*. (Tokyo: Nobunkyo).
- Imin, N., Kerim, T., Rolfe, B.G., and Weinman, J.J.** (2004). Effect of early cold stress on the maturation of rice anthers. *Proteomics* **4**, 1873–1882.
- Inoue, N., Hess, K.D., Moreadith, R.W., Richardson, L.L., Handel, M.A., Watson, M.L., and Zinn, A.R.** (1999). New gene family defined by MORC, a nuclear protein required for mouse spermatogenesis. *Hum. Mol. Genet.* **8**, 1201–1207.
- Ishiguro, S., and Nakamura, K.** (1994). Characterization of a cDNA encoding a novel DNA-binding protein, SPF1, that recognizes SP8 sequences in the 5' upstream regions of genes coding for sporamin and β -amylase from sweet potato. *Mol. Gen. Genet.* **244**, 563–571.
- Jefferson, R.A., Kavanagh, T.A., and Bevan, M.W.** (1987). GUS fusions: Beta-glucuronidase as a sensitive and versatile gene fusion marker in higher plants. *EMBO J.* **6**, 3901–3907.
- Jeon, J.S., et al.** (2000). T-DNA insertional mutagenesis for functional genomics in rice. *Plant J.* **22**, 561–570.
- Jeong, D.H., An, S., Kang, H.G., Moon, S., Han, J.J., Park, S., Lee, H.S., An, K., and An, G.** (2002). T-DNA insertional mutagenesis for activation tagging in rice. *Plant Physiol.* **130**, 1636–1644.
- Jin, J.B., Kim, Y.A., Kim, S.J., Lee, S.H., Kim, D.H., Cheong, G.-W., and Hwang, I.** (2001). A new dynamin-like protein, ADL6, is involved in trafficking from the *trans*-Golgi network to the central vacuole in *Arabidopsis*. *Plant Cell* **13**, 1511–1525.
- Johnson, C.S., Kolevski, B., and Smyth, D.R.** (2002). TRANSPARENT TESTA GLABRA2, a trichome and seed coat development gene of *Arabidopsis*, encodes a WRKY transcription factor. *Plant Cell* **14**, 1359–1375.
- Jung, K.H., Hur, J., Ryu, C.H., Choi, Y., Chung, Y.Y., Miyao, A., Hirochika, H., and An, G.** (2003). Characterization of a rice chlorophyll-deficient mutant using the T-DNA gene-trap system. *Plant Cell Physiol.* **44**, 463–472.
- Kang, H.G., Jeon, J.S., Lee, S., and An, G.** (1998). Identification of class B and class C floral organ identity genes from rice plants. *Plant Mol. Biol.* **38**, 1021–1029.
- Kapoor, S., Kobayashi, A., and Takatsuji, H.** (2002). Silencing of the tapetum-specific zinc finger gene TAZ1 causes premature degeneration of tapetum and pollen abortion in petunia. *Plant Cell* **14**, 2353–2367.
- Kim, C.Y., and Zhang, S.** (2004). Activation of a mitogen-activated protein kinase cascade induces WRKY family of transcription factors and defense genes in tobacco. *Plant J.* **38**, 142–151.
- Koroleva, O.A., Tomlinson, M., Parinyapong, P., Sakvarelidze, L., Leader, D., Shaw, P., and Doonan, J.H.** (2004). CycD1, a putative G1 cyclin from *Antirrhinum majus*, accelerates the cell cycle in cultured tobacco BY-2 cells by enhancing both G1/S entry and progression through S and G2 phases. *Plant Cell* **16**, 2364–2379.
- Lan, L., et al.** (2004). Monitoring of gene expression profiles and isolation of candidate genes involved in pollination and fertilization in rice (*Oryza sativa* L.) with a 10K cDNA microarray. *Plant Mol. Biol.* **54**, 471–487.
- Lee, S., Jung, K.H., An, G., and Chung, Y.Y.** (2004). Isolation and characterization of a rice cysteine protease gene, OsCP1, using T-DNA gene-trap system. *Plant Mol. Biol.* **54**, 755–765.
- Lee, S., Kim, J., Son, J.S., Nam, J., Jeong, D.H., Lee, K., Jang, S., Yoo, J., Lee, J., Lee, D.Y., Kang, H.G., and An, G.** (2003). Systematic reverse genetic screening of T-DNA tagged genes in rice for functional genomic analyses: MADS-box genes as a test case. *Plant Cell Physiol.* **44**, 1403–1411.
- Liu, X.C., and Dickinson, H.G.** (1989). Cellular energy levels and their effect on male cell abortion in cytoplasmically male sterile lines of *Petunia hybrida*. *Sex. Plant Reprod.* **2**, 167–172.
- Liu, Y.G., Mitsukawa, N., Oosumi, T., and Whittier, R.F.** (1995). Efficient isolation and mapping of *Arabidopsis thaliana* T-DNA insert junctions by thermal asymmetric interlaced PCR. *Plant J.* **8**, 457–463.
- McCormick, S.** (1993). Male gametophyte development. *Plant Cell* **5**, 1265–1275.
- Nonomura, K., Nakano, M., Fukuda, T., Eiguchi, M., Miyao, A., Hirochika, H., and Kurata, N.** (2004a). The novel gene HOMOLOGOUS PAIRING ABERRATION IN RICE MEIOSIS1 of rice encodes a putative coiled-coil protein required for homologous chromosome pairing in meiosis. *Plant Cell* **16**, 1008–1020.
- Nonomura, K.I., Miyoshi, K., Eiguchi, M., Suzuki, T., Miyao, A., Hirochika, H., and Kurata, N.** (2003). The *MSP1* gene is necessary to restrict the number of cells entering into male and female sporogenesis and to initiate anther wall formation in rice. *Plant Cell* **15**, 1728–1739.
- Nonomura, K.I., Nakano, M., Murata, K., Miyoshi, K., Eiguchi, M., Miyao, A., Hirochika, H., and Kurata, N.** (2004b). An insertional mutation in the rice *PAIR2* gene, the ortholog of *Arabidopsis* *ASY1*, results in a defect in homologous chromosome pairing during meiosis. *Mol. Genet. Genomics* **271**, 121–129.
- Raghavan, V.** (1981). A transient accumulation of poly(A)-containing RNA in the tapetum of *Hyoscyamus niger* during microsporogenesis. *Dev. Biol.* **81**, 342–348.
- Raghavan, V.** (1989). mRNAs and a cloned histone gene are differentially expressed during anther and pollen development in rice (*Oryza sativa* L.). *J. Cell Sci.* **92**, 217–229.
- Ryu, C.H., You, J.H., Kang, H.G., Hur, J., Kim, Y.H., Han, M.J., An, K., Chung, B.C., Lee, C.H., and An, G.** (2004). Generation of T-DNA tagging lines with a bidirectional gene trap vector and the establishment of an insertion-site database. *Plant Mol. Biol.* **54**, 489–502.
- Sanders, P.M., Bui, A.Q., Koen, W., McIntire, K.N., Hsu, Y.-C., Lee, P.Y., Truong, M., Beals, T.P., and Goldberg, R.B.** (1999). Anther developmental defects in *Arabidopsis thaliana* male-sterile mutants. *Sex. Plant Reprod.* **11**, 297–322.
- Sasaki, T., Matsumoto, T., Antonio, B.A., and Nagamura, Y.** (2005). From mapping to sequencing, post-sequencing and beyond. *Plant Cell Physiol.* **46**, 3–13.
- Schieffhale, U., Balasubramanian, S., Sieber, P., Chevalier, D., Wisman, E., and Schneitz, K.** (1999). Molecular analysis of NOZZLE, a gene involved in pattern formation and early sporogenesis during sex organ development in *Arabidopsis thaliana*. *Proc. Natl. Acad. Sci. USA* **96**, 11664–11669.
- Scott, R.J., Spielman, M., and Dickinson, H.G.** (2004). Stamen structure and function. *Plant Cell* **16** (suppl.), S46–S60.
- Solano, R., Nieto, C., Avila, J., Canas, L., Diaz, I., and Paz-Ares, J.** (1995). Dual DNA binding specificity of a petal epidermis-specific MYB transcription factor (MYB.Ph3) from *Petunia hybrida*. *EMBO J.* **14**, 1773–1784.
- Sorensen, A., Guerineau, F., Canales-Holzeis, C., Dickinson, H.G., and Scott, R.J.** (2002). A novel extinction screen in *Arabidopsis*

- thaliana* identifies mutant plants defective in early microsporangial development. *Plant J.* **29**, 581–594.
- Sorensen, A.-M., Kröber, S., Unte, U.S., Huijser, P., Dekker, K., and Saedler, H.** (2003). The *Arabidopsis* *ABORTED MICROSPORES (AMS)* gene encodes a MYC class transcription factor. *Plant J.* **33**, 413–423.
- Sun, C., Palmqvist, S., Olsson, H., Boren, M., Ahlandsberg, S., and Jansson, C.** (2003). A novel WRKY transcription factor, *SUSIBA2*, participates in sugar signaling in barley by binding to the sugar-responsive elements of the *iso1* promoter. *Plant Cell* **15**, 2076–2092.
- Toledo-Ortiz, G., Huq, E., and Quail, P.H.** (2003). The *Arabidopsis* basic/helix-loop-helix transcription factor family. *Plant Cell* **15**, 1749–1770.
- Truernit, E., Stadler, R., Baier, K., and Sauer, N.** (1999). A male gametophyte-specific monosaccharide transporter in *Arabidopsis*. *Plant J.* **17**, 191–201.
- Tsuchiya, T., Toriyama, K., Ejiri, S., and Hinata, K.** (1994). Molecular characterization of rice genes specially expressed in the anther tapetum. *Plant Mol. Biol.* **26**, 1737–1746.
- Vierstra, R.D.** (2003). The ubiquitin/26S proteasome pathway, the complex last chapter in the life of many plant proteins. *Trends Plant Sci.* **8**, 135–142.
- Wilson, Z.A., Morroll, S.M., Dawson, J., Swarup, R., and Tighe, P.J.** (2001). The *Arabidopsis* *MALE STERILITY1 (MS1)* gene is a transcriptional regulator of male gametogenesis, with homology to the PHD-finger family of transcription factors. *Plant J.* **28**, 27–39.
- Yamaguchi, T., Nakayama, K., Hayashi, T., Yazaki, J., Kishimoto, N., Kikuchi, S., and Koike, S.** (2004). cDNA microarray analysis of rice anther genes under chilling stress at the microsporogenesis stage revealed two genes with DNA transposon *Castaway* in the 5′-flanking region. *Biosci. Biotechnol. Biochem.* **68**, 1315–1323.
- Yang, M., Hu, Y., Lodhi, M., McCombie, W.R., and Ma, H.** (1999a). The *Arabidopsis* *SKP1-LIKE1* gene is essential for male meiosis and may control homologue separation. *Proc. Natl. Acad. Sci. USA* **96**, 11416–11421.
- Yang, S.-L., Xie, L.-F., Mao, H.-Z., Pauh, C.S., Yang, W.-C., Jiang, L., Sundaresan, V., and Ye, D.** (2003a). *TAPETUM DETERMINANT1* is required for cell specialization in the *Arabidopsis* anther. *Plant Cell* **15**, 2792–2804.
- Yang, W.C., Ye, D., Xu, J., and Sundaresan, V.** (1999b). The *SPOROCTELESS* gene of *Arabidopsis* is required for initiation of sporogenesis and encodes a novel nuclear protein. *Genes Dev.* **13**, 2108–2117.
- Yang, X., Makaroff, C.A., and Ma, H.** (2003b). The *Arabidopsis* *MALE MEIOCYTE DEATH1* gene encodes a PHD-finger protein that is required for male meiosis. *Plant Cell* **15**, 1281–1295.
- Yang, Y.H., Dudoit, S., Luu, P., Lin, D.M., Peng, V., Ngai, J., and Speed, T.P.** (2002). Normalization for cDNA microarray data: A robust composite method addressing single and multiple slide systematic variation. *Nucleic Acids Res.* **30**, e15.
- Zhang, F., Gonzalez, A., Zhao, M., Payne, C.T., and Lloyd, A.** (2003). A network of redundant bHLH proteins functions in all TTG1-dependent pathways of *Arabidopsis*. *Development* **130**, 4859–4869.
- Zhao, D.Z., Wang, G.F., Speal, B., and Ma, H.** (2002). The excess microsporocytes1 gene encodes a putative leucine-rich repeat receptor protein kinase that controls somatic and reproductive cell fates in the *Arabidopsis* anther. *Genes Dev.* **16**, 2021–2031.
- Zimmermann, I.M., Heim, M.A., Weisshaar, B., and Uhrig, J.F.** (2004). Comprehensive identification of *Arabidopsis thaliana* MYB transcription factors interacting with R/B-like BHLH proteins. *Plant J.* **40**, 22–34.